General Disclaimer

One or more of the Following Statements may affect this Document

- This document has been reproduced from the best copy furnished by the organizational source. It is being released in the interest of making available as much information as possible.

- This document may contain data, which exceeds the sheet parameters. It was furnished in this condition by the organizational source and is the best copy available.

- This document may contain tone-on-tone or color graphs, charts and/or pictures, which have been reproduced in black and white.

- This document is paginated as submitted by the original source.

- Portions of this document are not fully legible due to the historical nature of some of the material. However, it is the best reproduction available from the original submission.

ORIGINAL PAGE IS
OF POOR QUALITY

AERODYNAMIC CHARACTERISTICS OF
AN 11-PERCENT-THICK SYMMETRICAL
SUPERCRITICAL AIRFOIL AT
MACH NUMBERS BETWEEN 0.30 AND 0.85

by James A. Blackwell, Jr.

Langley Research Center
Langley Station, Hampton, Va.

ORIGINAL PAGE IS
OF POOR QUALITY

AERODYNAMIC CHARACTERISTICS OF AN

11-PERCENT-THICK SYMMETRICAL SUPERCRITICAL AIRFOIL

AT MACH NUMBERS BETWEEN 0.30 AND 0.85

By James A. Blackwell, Jr.

Langley Research Center
Langley Station, Hampton, Va.

AERODYNAMIC CHARACTERISTICS OF AN

11-PERCENT-THICK SYMMETRICAL SUPERCRITICAL AIRFOIL

AT MACH NUMBERS BETWEEN 0.30 AND 0.85*

By James A. Blackwell, Jr.
Langley Research Center

SUMMARY

An investigation was conducted in the Langley 8-foot transonic pressure tunnel over a Mach number range of 0.30 to 0.85 to determine the aerodynamic characteristics of an 11-percent-thick symmetrical supercritical airfoil. The Reynolds number of the tests, based on the airfoil chord, varied with Mach number over a range of 3.60×10^6 to 7.74×10^6. The geometric angle of attack varied from -0.5° to 10.5°.

The results of the investigation indicate that the abrupt drag rise for the supercritical airfoil at zero-normal-force conditions occurs at a Mach number just above 0.82. The corresponding drag-rise Mach number for a conventional NACA 0012 airfoil is approximately 0.70. At zero-normal-force conditions, the level of supervelocity over the supercritical airfoil is considerably reduced from that for the NACA 0012 airfoil. Also, the shock wave for the supercritical airfoil is substantially weaker than that for the NACA 0012 airfoil. For a Mach number of 0.82 and zero normal force, the flow over the present airfoil is supercritical; however, there is no discernible shock wave in the flow, indicating near-isentropic recompression.

At moderate-normal-force conditions, the supercritical airfoil has only a slight improvement over the conventional NACA 0012 airfoil in drag-rise Mach number.

INTRODUCTION

The design of airfoil sections for helicopter rotor blades has progressed very slowly over the past few years. This is primarily because of the severe operating requirements for helicopter sections. The section must perform well at (1) high-transonic Mach numbers for low lift coefficients, (2) high subsonic speeds for moderate lift coefficients, and (3) low-subsonic Mach numbers for maximum lift. The sections are also restricted to little or no camber as a result of pitching-moment considerations.

Presently, sections such as the NACA 4- and 5-digit series (or modifications thereof) are being used for helicopter blades. For advanced helicopter systems, higher forward speeds with resulting higher tip speeds are required. This results in a large proportion of the advancing blade being immersed in transonic flow. Use of the afore-mentioned sections in these advanced helicopter systems would result in large transonic drag penalties.

Considerable progress has been made in recent years in transonic airfoil aerody-namics. In particular, marked improvements have been found for cambered supercritical airfoils for application to transport aircraft (refs. 1 and 2). One of the primary results of these studies is the large delay in the transonic drag-rise Mach number obtained through proper design.

These results have prompted the NASA to take renewed interest in the development of advanced airfoils for rotor blades with special emphasis on the performance in the high-transonic—low-lift range. To determine if the gains shown for cambered transonic air-foils could be realized in symmetrical sections for helicopter application, wind-tunnel tests were made on a symmetrical "supercritical" airfoil incorporating the supercritical design concepts of references 1 and 2.

The present investigation was performed in the Langley 8-foot transonic pressure tunnel over a Mach number range of 0.30 to 0.85. The Reynolds numbers of the tests varied with Mach number over a range of 3.60×10^6 to 7.74×10^6. The geometrical angle of attack varied from -0.5° to 10.5°.

SYMBOLS

c_d section drag coefficient, $\sum \dfrac{c_d{}' \, \Delta z}{c}$

$c_d{}'$ point drag coefficient (ref. 3)

c_m section pitching-moment coefficient, $\sum_{l.s.} \dfrac{C_p \, \Delta x}{c}\left(0.25 - \dfrac{x}{c}\right) - \sum_{u.s.} \dfrac{C_p \, \Delta x}{c}\left(0.25 - \dfrac{x}{c}\right)$

or $\displaystyle\int_{l.s.} C_p\left(0.25 - \dfrac{x}{c}\right)d\left(\dfrac{x}{c}\right) - \int_{u.s.} C_p\left(0.25 - \dfrac{x}{c}\right)d\left(\dfrac{x}{c}\right)$

c_n section normal-force coefficient, $\sum_{l.s.} \dfrac{C_p \, \Delta x}{c} - \sum_{u.s.} \dfrac{C_p \, \Delta x}{c}$

C_p pressure coefficient, $\dfrac{p - p_\infty}{q_\infty}$

$C_{p,sonic}$ pressure coefficient corresponding to local Mach number of 1.0

c   chord of airfoil, in. (cm)

M   free-stream Mach number

p   local static pressure at a point on airfoil, lb/ft^2 (N/m^2)

p_∞ static pressure in undisturbed stream, lb/ft^2 (N/m^2)

Δp_t total pressure loss, lb/ft^2 (N/m^2)

q_∞ dynamic pressure in undisturbed stream, lb/ft^2 $(N/m2)$

r   airfoil-leading-edge radius, in. (cm)

R   Reynolds number based on airfoil chord

t   airfoil thickness, in. (cm)

x   ordinate along airfoil reference line measured from airfoil leading edge, in. (cm)

y   ordinate vertical to airfoil reference line, in. (cm)

y' slope of airfoil surface, dy/dx

z   vertical distance in wake profile, in. (cm)

α angle of attack of airfoil reference line, deg

Abbreviations:

l.s.   lower surface

u.s.   upper surface

MODEL DESIGN

When the flow over the airfoil exceeds a local Mach number of 1, a region of super-
sonic flow extends vertically over the airfoil (fig. 1). This supersonic region usually
culminates in a shock wave. As the free-stream Mach number is increased, the shock
wave for conventional helicopter sections becomes increasingly stronger with associated
increases in drag. Ultimately, the shock wave becomes strong enough to induce the
boundary layer to separate, resulting in the abrupt drag rise. These increases in drag
severely curtail the performance of conventional sections.

The airfoil shape that is proposed herein is intended to reduce the strength of the
shock wave significantly and, hence, the tendency of shock-induced boundary-layer separa-
tion. An airfoil so designed would reduce the creeping drag rise and delay the abrupt
drag rise well beyond the critical Mach number.

In the present approach, the strength of the shock wave is primarily reduced by a
careful profiling of the airfoil to reduce the level of supervelocity upstream of the shock
wave. Physically, this may be done by requiring a large leading-edge radius and by
requiring the airfoil surface rearward of the leading edge to be of small curvature. These
requirements result in a high rate of curvature at the intersection of the nose radius and
the airfoil contour. This high rate of curvature produces a large velocity peak at the
leading edge. The "peaky" velocity distribution generates strong expansion waves which
strike the sonic line. Through proper contouring, these expansion waves will reflect from
the sonic line as Mach number decreasing compression waves in the vicinity of the shock.
In figure 1 this effect is illustrated schematically for a single expansion wave originating
near the leading edge of the airfoil. Following this procedure, the strength of the shock
wave can be diminished to rear-isentropic recompression. (See ref. 4 for a full discus-
sion of the subject.)

The contouring of the region aft of the airfoil crest is done such that the level of
supervelocity generally remains constant as the shock wave passes rearward over the
crest. This prohibits the strength of the shock wave from increasing. The physical
requirement to produce this type of pressure distribution is a shape that progressively
increases in slope and curvature proceeding from the airfoil crest to the trailing edge.

It is well known that a large airfoil-leading-edge radius is favorable for generating
maximum normal force at low subsonic speeds. Therefore, it appears that the shape
required for optimizing the transonic normal-force characteristics is compatible with
the shape required for obtaining maximum normal force at low subsonic speeds.

An airfoil that has been designed on the basis of the aforementioned requirements is
presented in figure 2. The slope diagram for the airfoil is presented in figure 3. The
ordinates and slopes are tabulated in table I.

The shape is governed by the following formulas:

$$0.007 \leq \frac{x}{c} \leq 0.400$$

$$\left(\frac{y}{c}\right) = 0.0550 - 0.112107\left(\sqrt{0.433} - \sqrt{\frac{x}{c} - 0.002124}\right)^2$$

$$0.403 \leq \frac{x}{c} \leq 1.000$$

$$\left(\frac{y}{c}\right) = \left[0.05482 - 0.1127955\left(\frac{x}{c} - 0.403\right)^2 - 0.249488\left(\frac{x}{c} - 0.403\right)^{5.5}\right]$$

$$\frac{r}{c} = 0.022275$$

The model chord was 24.8 inches (63.0 cm) in length.

In figure 4 the thickness distribution of the supercritical airfoil, the NACA 0011 airfoil, and the NACA 16-011 airfoil are compared. It can be seen that the present airfoil is similar to the NACA 0011 airfoil on the forepart of the airfoil and similar to the NACA 16-011 airfoil on the afterpart of the airfoil. The NACA 4-digit airfoil excels primarily at low-subsonic Mach numbers and at maximum normal-force coefficients; however, the high-transonic Mach number characteristics are very poor. The opposite trends are noted for the NACA 16-series airfoils. Comparing the shapes and characteristics of the three airfoils in figure 4, it appears that the present airfoil is an attempt to combine the best features of both airfoils.

APPARATUS AND MEASUREMENTS

Wind Tunnel

The investigation was performed in the Langley 8-foot transonic pressure tunnel. This facility is well suited to the investigation of two-dimensional models since it has solid side walls and slots in the upper and lower walls. The tunnel side walls act as end plates for the two-dimensional model, while the slots allow a development of the flow field in the vertical direction approaching that for free air (ref. 5). The slot opening at the position of the model was approximately 6 percent of the upper and lower walls.

The model was attached rigidly to the tunnel walls and completely spanned the width of the tunnel. The angle of attack of the model was changed manually by rotating the model about pivots in the tunnel side walls. The model was tested in an inverted position in order to make use of an existing angle-of-attack mount.

Transition Strips

Boundary-layer transition strips were located on both the upper and lower surfaces of the model at 0.05c unless otherwise indicated. The strips were 0.10 inch (0.25 cm) wide, consisting of No. 100 carborundum set in a plastic adhesive.

Surface-Pressure Measurements

The lift and pitching-moment forces acting on the airfoil were obtained from surface-pressure measurements. Surface pressures were measured with orifices located in a chordwise row at a spanwise station of 0.28c from the center line of the tunnel. Airfoil surface pressures were measured with the use of electronically actuated pressure-scanning-valve units. The maximum range of the transducers in the valves was ± 10 lb/in^2 (68 947 N/m^2).

Wake Measurements

The drag forces acting on the airfoils were derived from vertical variations of the wake total and static pressures measured with the rake shown in figure 5. The measurement station of the rake was approximately 1 chord length rearward of the trailing edge of the airfoil. The total-pressure tubes were closely spaced (see fig. 5) in the region of the wake associated with skin-friction boundary-layer losses. In this area, these tubes were flattened horizontally. Outside this region, the tube spacing progressively widened. The static-pressure tubes were distributed as shown in figure 5. The rake was attached to the conventional center-line sting mount of the Langley 8-foot transonic pressure tunnel. During the investigation, the rake was moved vertically to center the close concentration of tubes on the boundary-layer wake.

The total pressure and static pressures were measured with the use of electronically actuated pressure scanning valves. The maximum range of the gage in the valve connected to total-pressure tubes intended to measure losses in the boundary-layer wake was 5 lb/in^2 (34 474 N/m^2); the corresponding range for measuring shock losses was 1 lb/in^2 (6895 N/m^2), and that for the static pressures was 1 lb/in^2 (6895 N/m^2).

TEST CONDITIONS

The investigation was conducted over a Mach number range of 0.30 to 0.85. The Reynolds numbers of the tests varied with Mach number over a range of 3.60×10^6 to 7.74×10^6 (fig. 6) based on the model chord. The geometric angle of attack varied from -0.5° to 10.5°. The total temperature was held constant at approximately 580° R (322° K).

REDUCTION OF DATA AND CORRECTIONS

Calculation of c_n and c_m

The section normal-force and section pitching-moment coefficients were obtained by machine summation of the local pressure coefficients measured at each orifice multiplied by an appropriate weighting factor. This procedure was checked by hand integration and was found to be accurate within 1 percent.

Calculation of c_d

To obtain a section drag coefficient from the total and static pressures behind the model, point drag coefficients for each of the total-pressure measurements have been computed by using the procedure of reference 3. These point values have been summed by machine using appropriate weighting factors. Because of the special spacing of the total-pressure tubes, the errors of the results obtained by the procedure are estimated to be less than 1 percent.

Corrections for Wind-Tunnel Wall Effects

The major effect of the wind-tunnel wall on the results presented herein is a substantial up-flow at the position of the inverted model so that the real aerodynamic angle of attack is significantly less than the geometric angle. The mean value of this up-flow at the midchord of the model, in degrees, as determined by the theory of reference 5, is 3.00 times the section normal-force coefficient. For the present investigation, wherein the lift, drag, and pitching-moment characteristics have been obtained by surface-pressure and wake measurements, this deviation has little effect on the validity of these results. It merely causes a change of the geometric angle of attack at which a given set of results are obtained. The angles of attack used in the results presented herein have not been corrected for this up-flow.

The theory of reference 5 indicates that the tunnel-wall blockage effect is small.

RESULTS

The results of this investigation have been reduced to coefficient form. Selected data representing these results are presented in the figures listed in the following table:

DISCUSSION

Normal-Force and Drag Characteristics

Zero normal force.- As indicated in figure 8 for nonlifting conditions, the supercritical airfoil experiences a shallow drag rise from a Mach number of 0.70 to 0.82. The Mach number for abrupt drag rise for the supercritical airfoil is approximately 0.12 higher than the drag-rise Mach number of approximately 0.70 for the NACA 0012 airfoil of reference 6. This represents a significant 17 percent increase in the abrupt-drag-rise Mach number.

The phenomena associated with these drag effects are provided by the pressure distributions of figure 10. The subcritical pressure distributions indicate the presence of a leading-edge velocity peak. As the Mach number is increased, the strong expansion waves from the leading edge reflect from the sonic line as compression waves (fig. 1) and cancel the expansion waves generated by the crest.

At a Mach number of 0.82 ($\alpha = 0^\circ$), the full compressive effect resulting from the leading-edge expansion waves is felt near the shock wave. This may be seen from the pressure distribution results (fig. 10(b)) and the oil-flow photographs (fig. 12) which indicate no discernible shock wave in the flow. Hence, the design goal of obtaining

near-isentropic recompression has been obtained. At a Mach number of 0.83, a slight increase in drag is shown in the wake surveys of figure 11, although the wave is still of insufficient strength to appear in the oil-flow photographs of figure 12. At M = 0.84, the shock moves rearward and increases in strength. In addition, the shock pressure rise and the steep pressure recovery near the trailing edge merge (fig. 10(b)), requiring the boundary layer to traverse two successive adverse gradients, thus leading to the significant increase in drag shown in figure 8. The shock now appears in the oil-flow pattern (fig. 12).

To indicate the success of this design approach in reducing the level of supervelocity over the airfoil and, hence, the strength of the shock wave, a comparison of the chordwise pressure distributions between the supercritical airfoil and the NACA 0012 airfoil are presented in figure 13 for a Mach number of 0.80 and $\alpha = 0^{\circ}$. For the example shown, the level of velocity is considerably reduced for the supercritical airfoil with respect to the NACA 0012 airfoil. Also, the shock wave for the supercritical airfoil is very weak in comparison to the strong shock wave for the NACA 0012 airfoil.

In figure 7(a) the effects of artificial boundary-layer transition on the section drag are indicated for zero normal force. As expected, there is a reduction in the drag with natural transition as a result of the increased extent of laminar flow on the airfoil.

Moderate normal force.- When the helicopter is in the hover condition, the typical blade experiences moderate normal-force coefficients (order of c_n = 0.4 to 0.6) and Mach numbers in range of 0.50 to 0.65. At moderate normal-force coefficients, it appears the crossover point in performance between the NACA 0012 airfoil and the supercritical airfoil (fig. 9) is just above a Mach number of 0.50. Therefore, in the moderate normal-force range, the supercritical airfoil has only a slight improvement over the NACA 0012 in drag-rise Mach number. The data for the NACA 0012 airfoil in figure 9 (taken from refs. 6 to 8) is represented by a band. Small variations in the results were indicated in these references due to the various differences in the test conditions and model conditions.

The performance of the supercritical airfoil at moderate normal forces and at low transonic Mach numbers was diminished as a result of the heavy emphasis placed on the zero-normal-force high-transonic Mach number condition. This can be seen by referring to figure 14. The subcritical leading-edge velocity peak generated at zero normal force (fig. 10(a)) increases substantially with angle of attack (fig. 14(a)). The velocity peak in figure 14(a) is of such magnitude that as the Mach number increases, a strong shock wave is generated at the leading edge and moves rearward (fig. 14(c)), thus precipitating the drag rise.

Improvements could probably be obtained in the drag-rise Mach number at moderate normal-force coefficients if the velocity peak were reduced. This could be achieved by slightly reducing the leading-edge radius; however, this would probably result in a trade-off with the high-transonic characteristics.

The effect of natural boundary-layer transition on the airfoil section characteristics is shown in figure 7 for moderate normal-force coefficients. For the limited data available with natural boundary-layer transition, there appears to be a reduction in normal force and an increase in the positive pitching moment in comparison with the data for the boundary layer fixed artificially near the leading edge. These effects can be explained by the differences indicated in the pressure distributions of figure 15. With natural boundary-layer transition, the boundary layer in the vicinity of the shock wave and at the airfoil trailing edge is much thinner (due to the increased chordwise extent of laminar flow) which results in a different boundary-layer shock interaction than would be obtained when the boundary-layer transition is fixed near the leading edge. In figure 15 it appears that for both cases a bubble forms just aft of the shock wave. The boundary-layer thickness in this area apparently affects the size and extent of this bubble. Also, since the overall boundary layer is thinner with natural transition, the flow is much more sensitive to the surface shape; hence, the velocities are increased over the lower surface, especially near the trailing edge of the airfoil. It is apparent from figure 15 that with natural transition the above effects generally combine to reduce the normal force and increase the positive pitching moment for a given angle of attack.

Maximum normal force.- In figures 7(b) and 16 the effect of angle of attack on the airfoil normal-force characteristics and chordwise pressure distribution, respectively, are shown at subsonic speeds. The maximum-normal-force characteristics in the range of Mach numbers from 0.40 to 0.50 appear to be considerably lower (by approximately 0.25 in c_n) in comparison with those for an NACA 0012 airfoil (refs. 6 to 8). However, the data at Mach numbers of 0.30 to 0.35 indicate that the maximum-normal-force characteristics significantly improve at these Mach numbers.

No conclusion may be reached from this series of tests as regards maximum normal force at the low subsonic Mach numbers since there is not sufficient data available.

Pitching-Moment Characteristics

It is desirable for an airfoil that will be used for a helicopter rotor blade to have near-zero pitching moments. The pitching moments (referenced to the quarter chord) shown in figure 7(c) are generally small in magnitude; however, for the subsonic Mach numbers an increase in positive pitching moment is indicated as the normal force is increased. The aerodynamic center at subsonic Mach numbers is approximately 0.2c. In comparison, the subsonic aerodynamic center of the NACA 0012 airfoil (ref. 8) is located at the airfoil quarter chord. The forward location of the supercritical airfoil aerodynamic center is primarily a result of the decreased load carried near the airfoil trailing edge with respect to conventional NACA 4-digit airfoils.

At transonic speeds the magnitude of the upper-surface leading-edge velocity peak diminishes (fig. 14) and, with increasing Mach number, forms a shock wave that moves rearward on the airfoil. The resulting pressure distribution at transonic speeds moves the aerodynamic center rearward to the quarter chord, reducing the pitching moments to near-zero values.

CONCLUSIONS

A wind-tunnel investigation has been conducted at Mach numbers from 0.30 to 0.85 on a two-dimensional 11-percent-thick symmetrical supercritical airfoil. Results of this investigation have indicated the following:

1. At zero-normal-force conditions the abrupt drag rise for the supercritical airfoil occurs at a Mach number just above 0.82. The corresponding drag-rise Mach number for a conventional NACA 0012 helicopter airfoil is approximately 0.70.

2. At zero-normal-force conditions, the level of supervelocity over the supercritical airfoil is considerably reduced from that for the NACA 0012 airfoil. Also, the shock wave for the supercritical airfoil is substantially weaker than that for the NACA 0012 airfoil.

3. For a Mach number of 0.82 and zero normal force, the flow over the present airfoil is supercritical; however, there is no discernible shock wave in the flow, indicating near-isentropic recompression.

4. At moderate-normal-force conditions, the supercritical airfoil has only a slight improvement over the conventional NACA 0012 airfoil in drag-rise Mach number.

Langley Research Center,
National Aeronautics and Space Administration,
Langley Station, Hampton, Va., April 24, 1969,
126-13-01-29-23.

REFERENCES

1. Whitcomb, Richard T.; and Clark, Larry R.: An Airfoil Shape for Efficient Flight at Supercritical Mach Numbers. NASA TM X-1109, 1965.

2. Whitcomb, Richard T.; and Blackwell, James A., Jr.: Status of Research on a Supercritical Wing. Conference on Aircraft Aerodynamics, NASA SP-124, 1966, pp. 367-381.

3. Baals, Donald D.; and Mourhess, Mary J.: Numerical Evaluation of the Wake-Survey Equations for Subsonic Flow Inlcuding the Effect of Energy Addition. NACA WR L-5, 1945. (Formerly NACA ARR L5H27.)

4. Lachmann, G. V., ed.: Boundary Layer and Flow Control. Vol. 2. Pergamon Press, 1961.

5. Davis, Don D.; and Moore, Dewey: Analytical Study of Blockage- and Lift-Interference Corrections for Slotted Tunnels Obtained by the Substitution of an Equivalent Homogeneous Boundary for the Discrete Slots. NACA RM L53E07b, 1953.

6. Tanner, Watson H.: Charts for Estimating Rotary Wing Performance in Hover and at High Forward Speeds. NASA CR-114, 1964.

7. Carpenter, Paul J.: Lift and Profile-Drag Characteristics of an NACA 0012 Airfoil Section as Derived From Measured Helicopter-Rotor Hovering Performance. NACA TN 4357, 1958.

8. Lizak, Alfred A.: Two-Dimensional Wind-Tunnel Tests of an H-34 Main Rotor Airfoil Section. TREC Tech. Rep. 60-53 (SER-58301), U.S. Army Transportation Res. Command (Fort Eustis, Va.), Sept. 1960.

TABLE I.- SUPERCRITICAL AIRFOIL ORDINATES AND SLOPES

x/c	y'	y/c
0	-----	0
0.0020	-----	0.009225
.0065243	1.0000	.015751
.0125	.6121	.020323
.0250	.3756	.026208
.0375	.2800	.030242
.050	.2250	.033373
.075	.1612	.038117
.100	.1237	.041643
.125	.0983	.044400
.150	.0797	.046615
.175	.0653	.048421
.200	.0537	.049905
.250	.0361	.052125
.300	.0231	.053588
.350	.0120	.054467
.400	.0007	.054783
.450	-.0106	.054571
.500	-.0219	.053758
.550	-.0334	.052376
.600	-.0454	.050410
.625	-.0517	.049198
.650	-.0583	.047824
.675	-.0653	.046281
.700	-.0728	.044556
.725	-.0810	.042635
.750	-.0900	.040499
.775	-.0999	.038127
.800	-.1110	.035492
.825	-.1235	.032564
.850	-.1375	.029306
.875	-.1533	.025676
.900	-.1711	.021625
.925	-.1914	.017099
.950	-.2143	.012034
.975	-.2401	.006361
1.000	-.2694	0
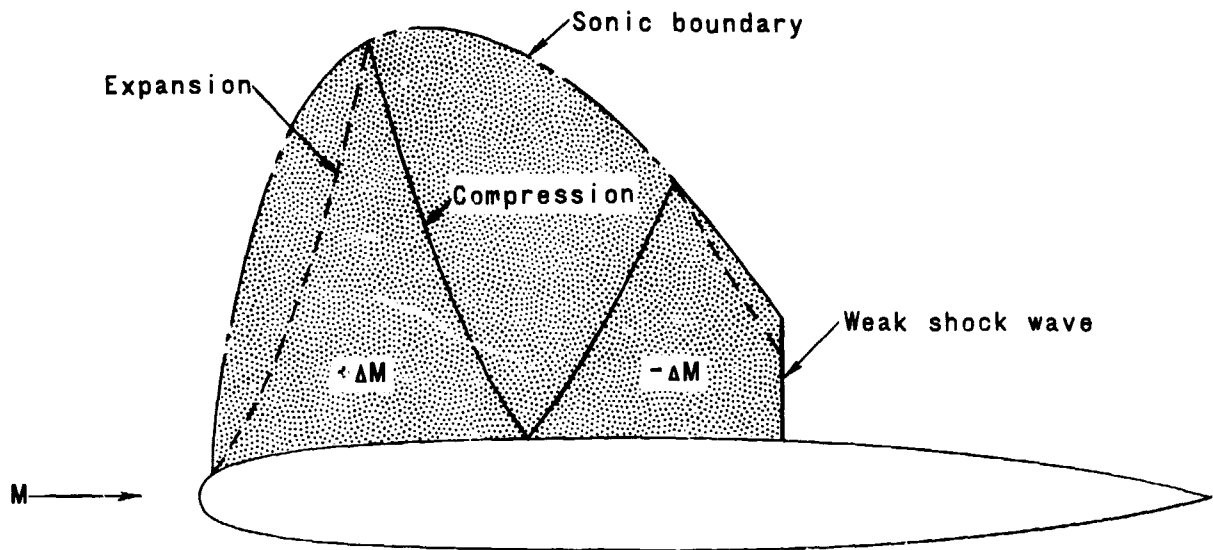
Schematic flow field
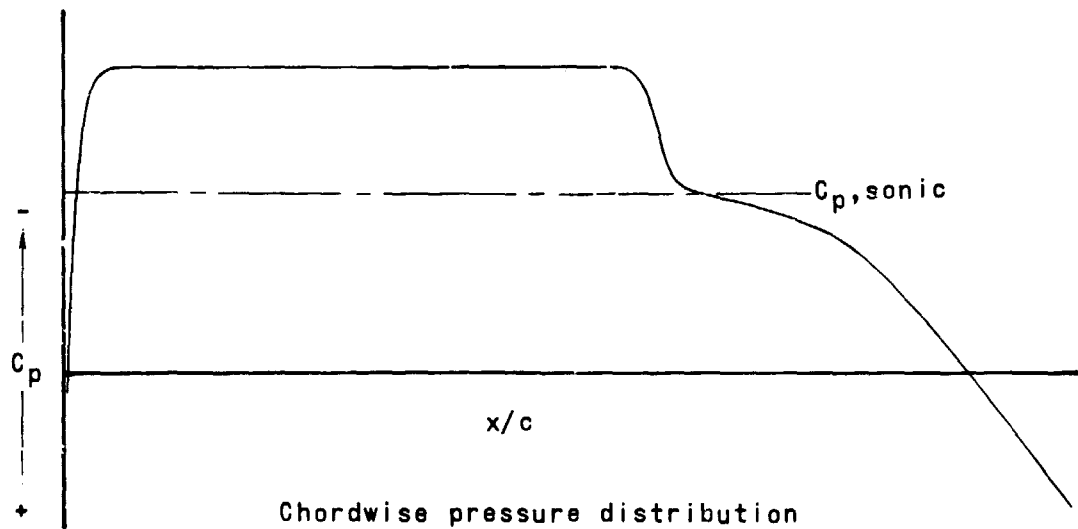
Chordwise pressure distribution

Figure 1.- Schematic illustration of supercritical phenomena at $\alpha = 0^0$ and $M = 0.83$.
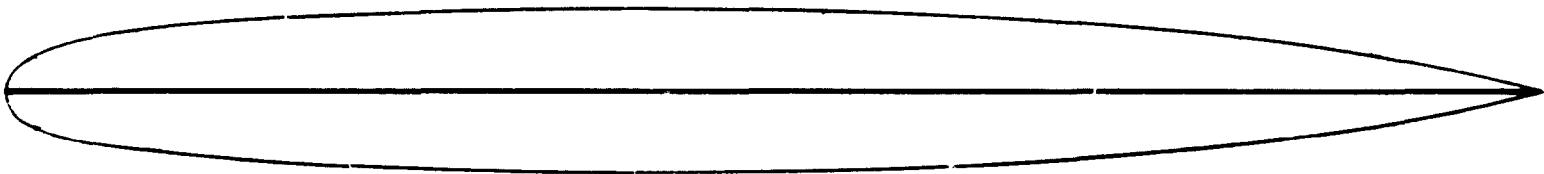
Figure 2.- Airfoil section shape.
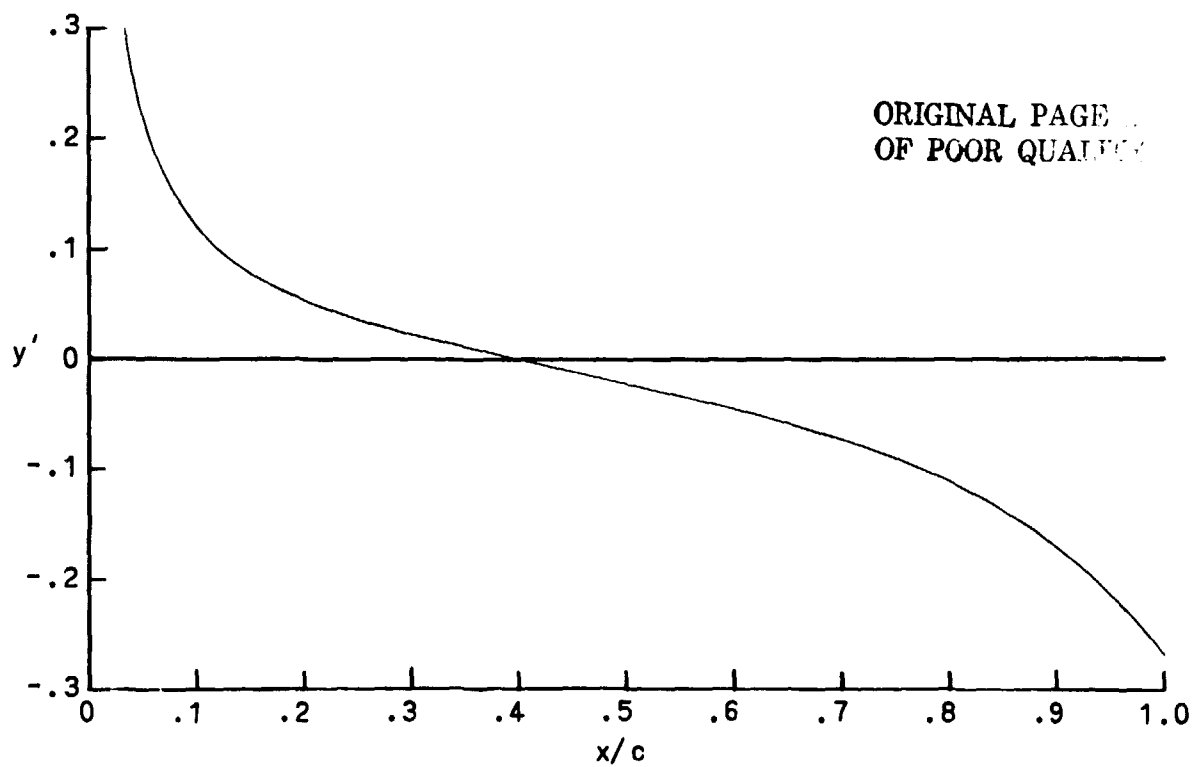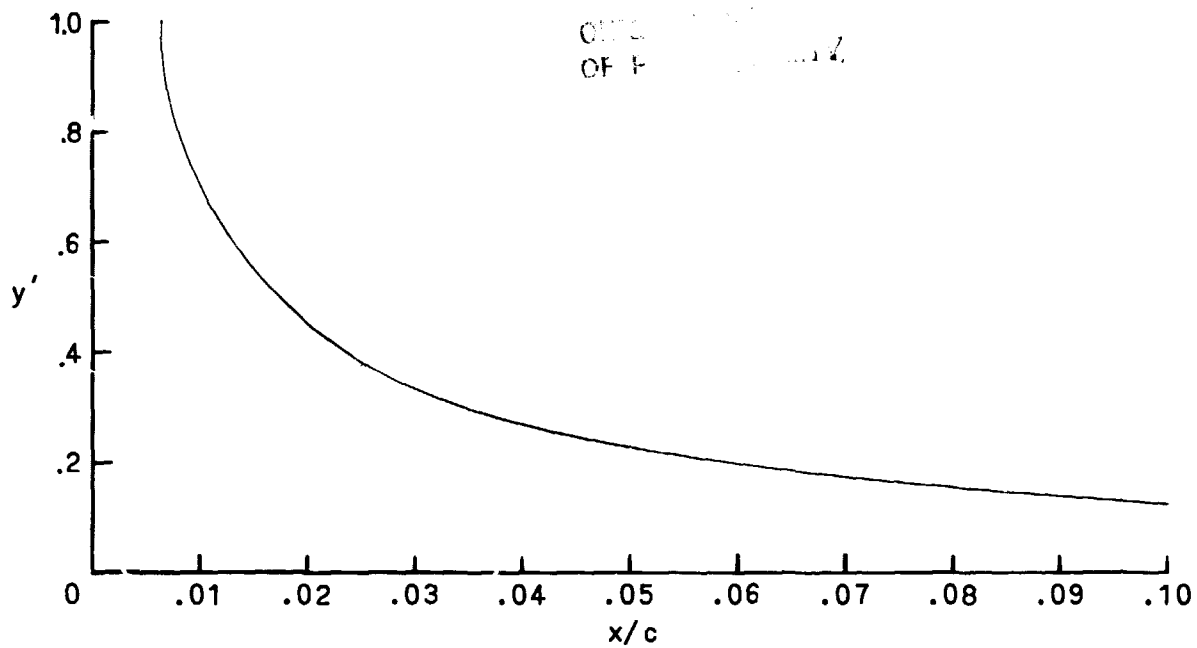
Figure 3.- Chordwise distribution of slopes.
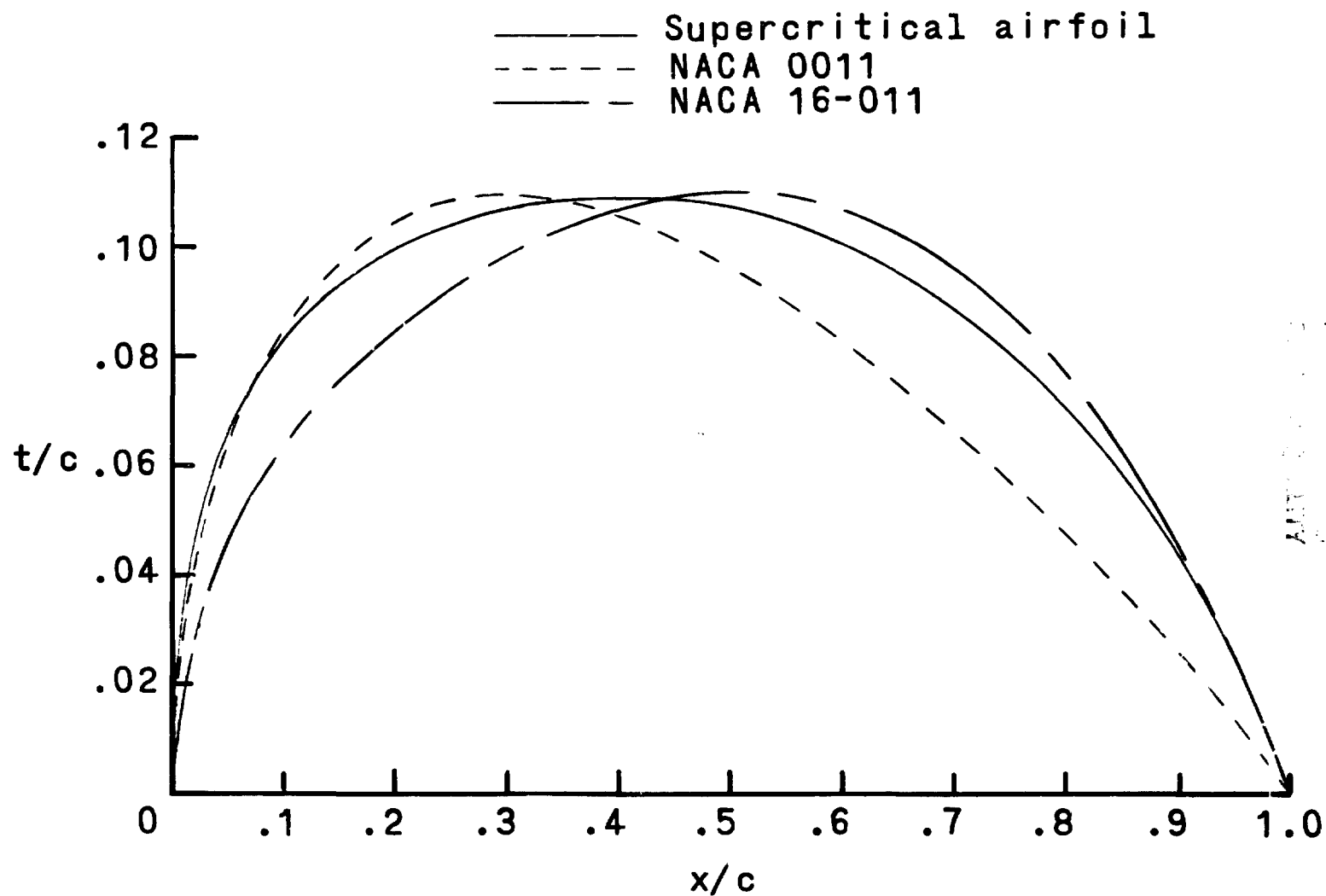
Figure 4.- Comparison of chordwise thickness distributions.

Airflow

Static-pressure probe

1.75
(4.45)
.50
(1.27)

6.00
(15.24)

Static-pressure probe

Tubes flattened and staggered

Tunnel ₵

Total-pressure probe

24.00
(60.96)

3.00
(7.62)

Diameter=0.06(.15)
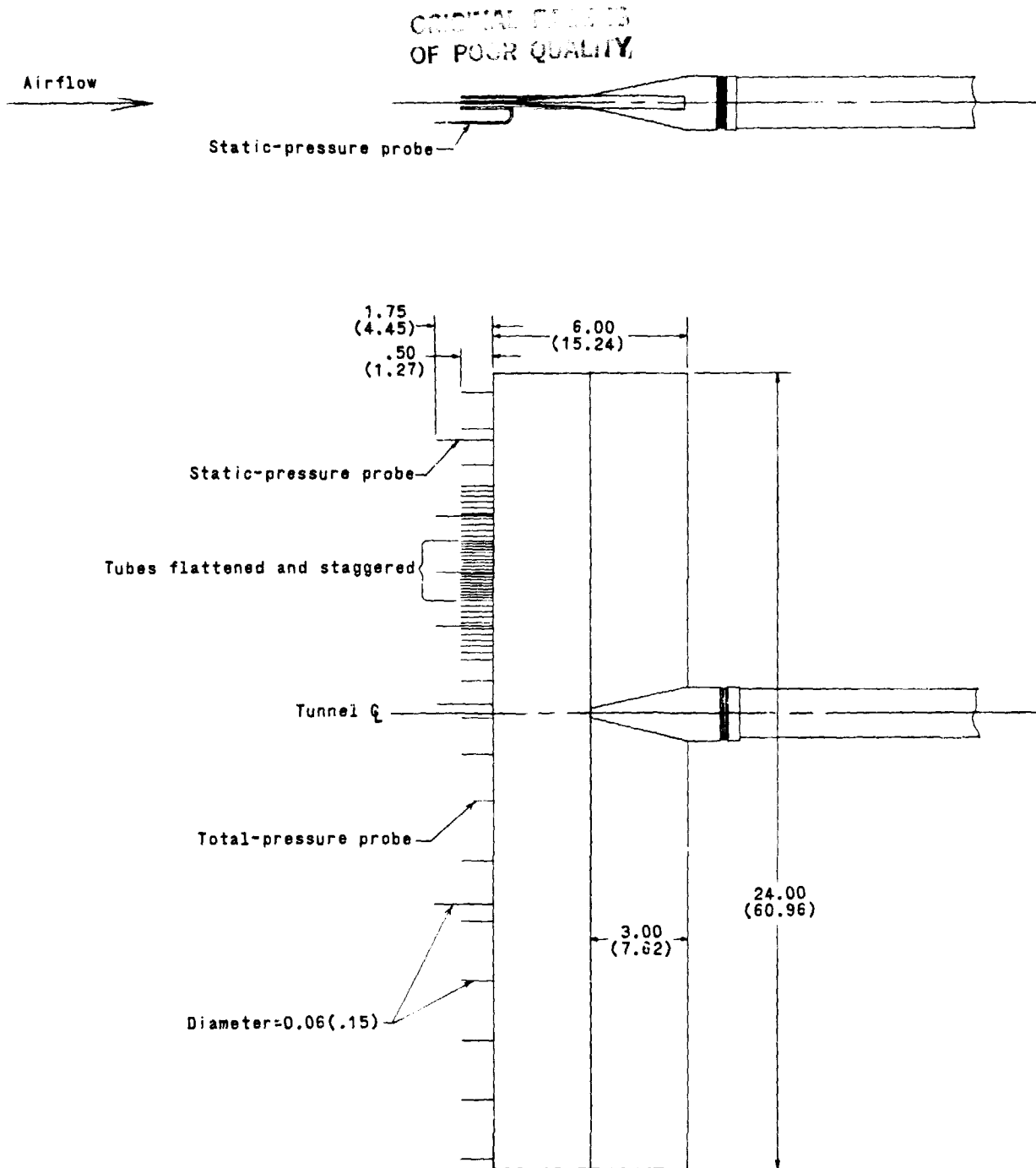
Figure 5.- Drawing of rake used for drag measurements. All dimensions in inches (centimeters in parentheses).
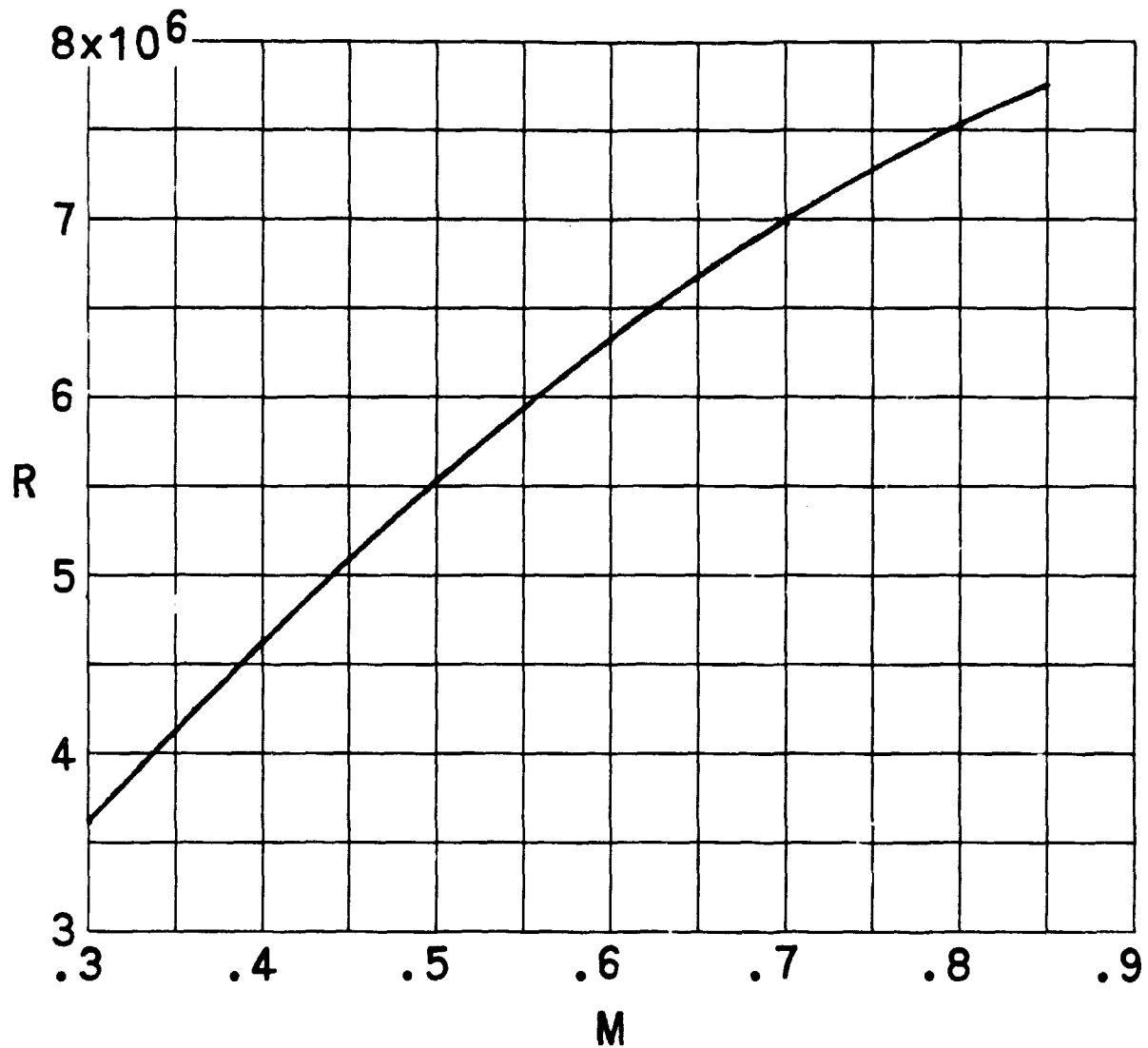
Figure 6.- Variation with Mach number of test Reynolds number.
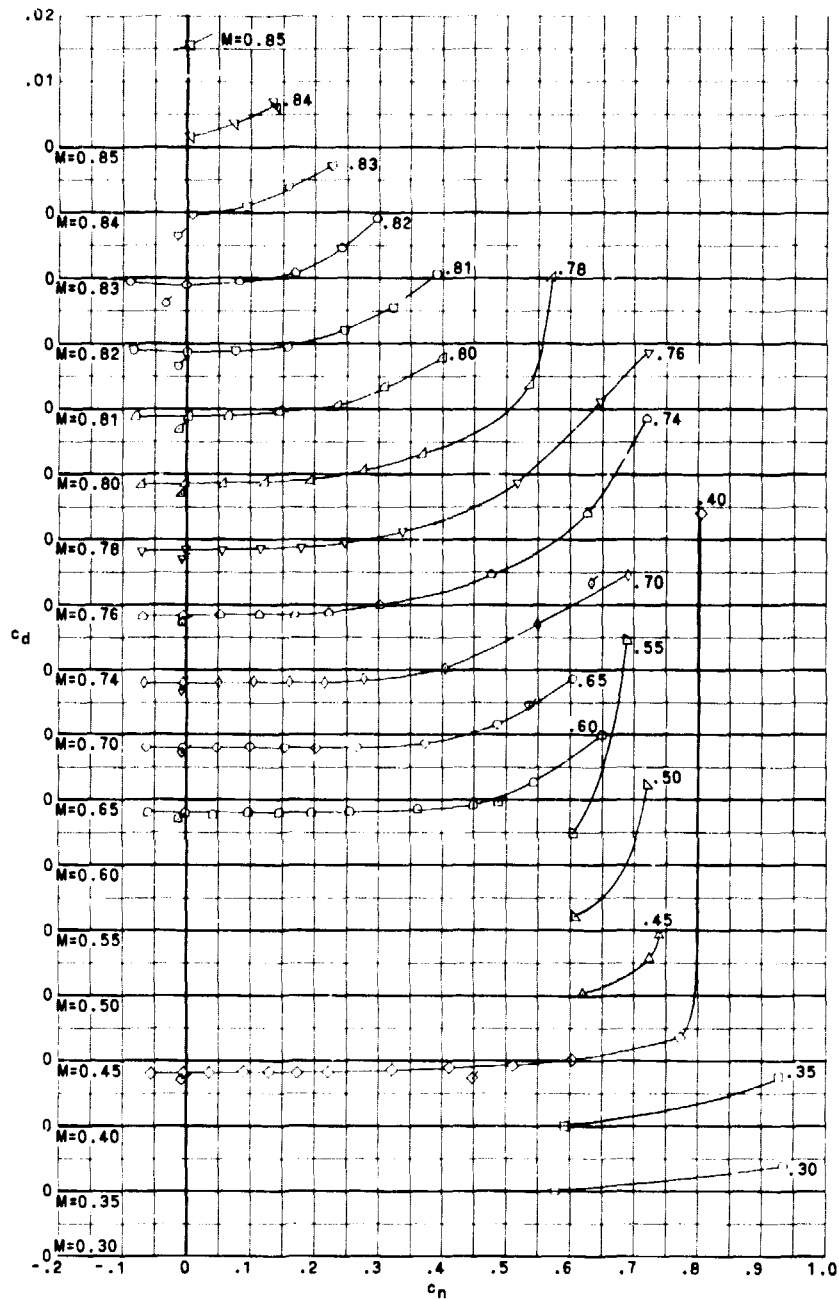
(a) Drag coefficient.

Figure 7.- Variation of section drag coefficient, angle of attack, and section pitching-moment coefficient with section normal-force coefficient for various Mach numbers. (Flagged symbols indicate transition off.)
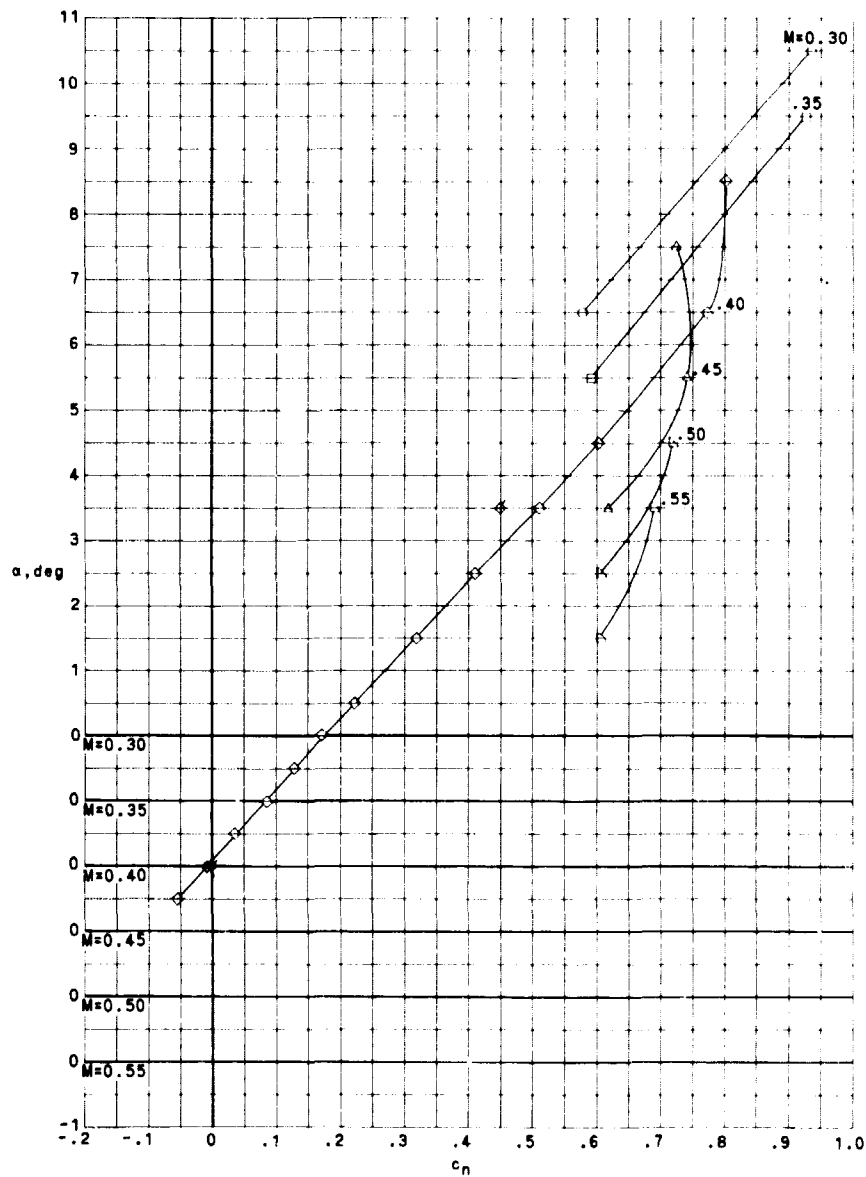
(b) Angle of attack.

Figure 7.- Continued.
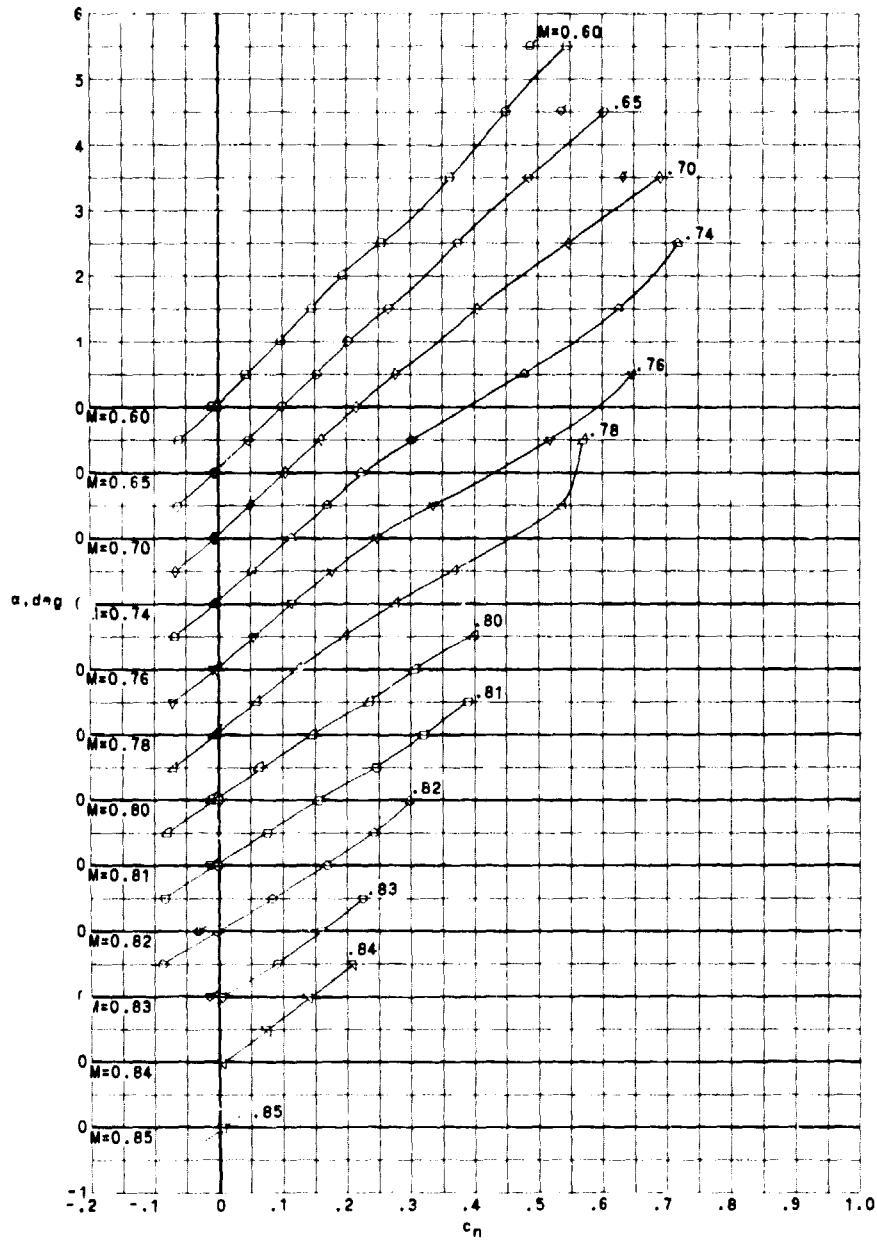
(b) Concluded.

Figure 7.- Continued.
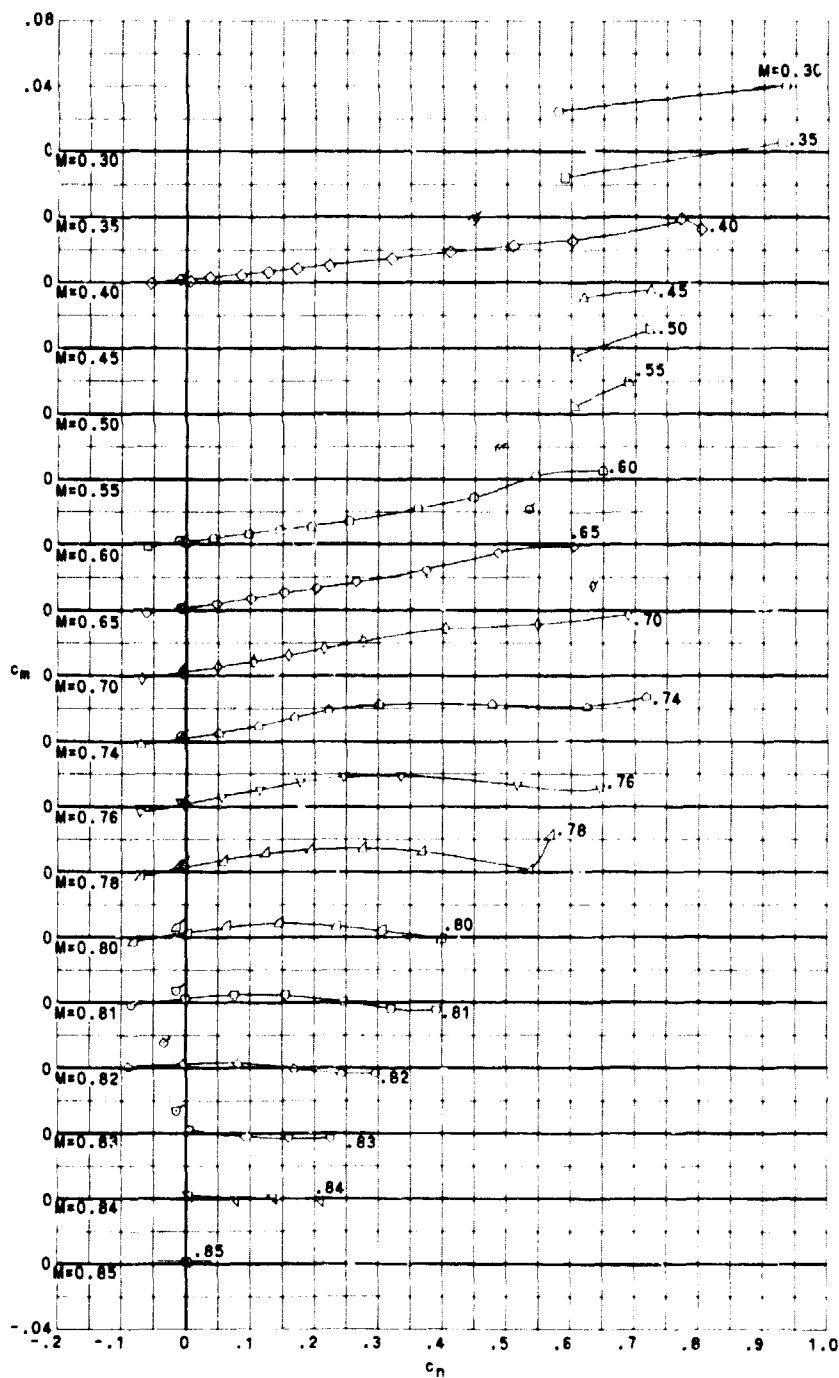
(c) Pitching-moment coefficient.

Figure 7.- Concluded.
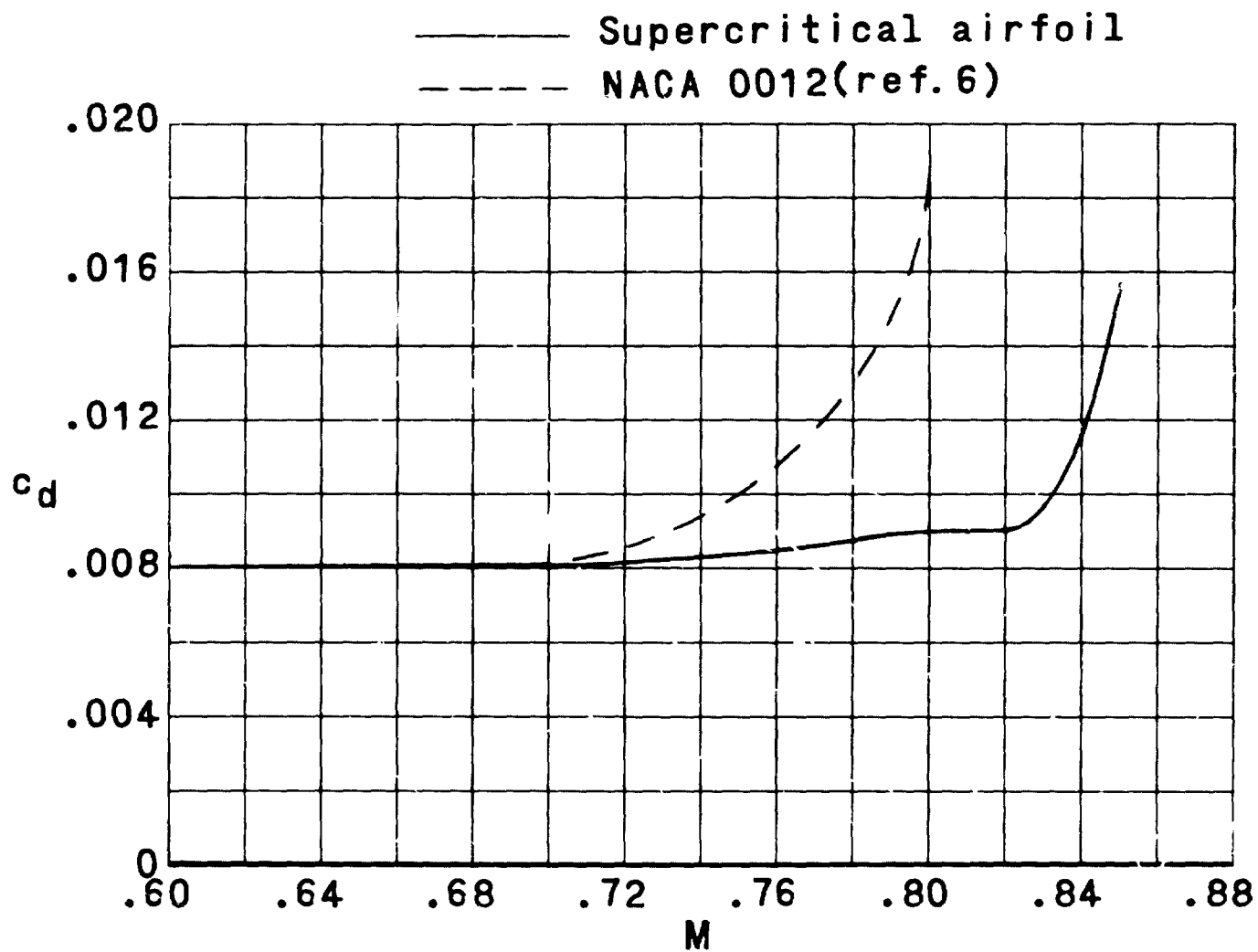
Figure 8.- Variation of section drag coefficients with Mach number for zero section normal-force coefficient.
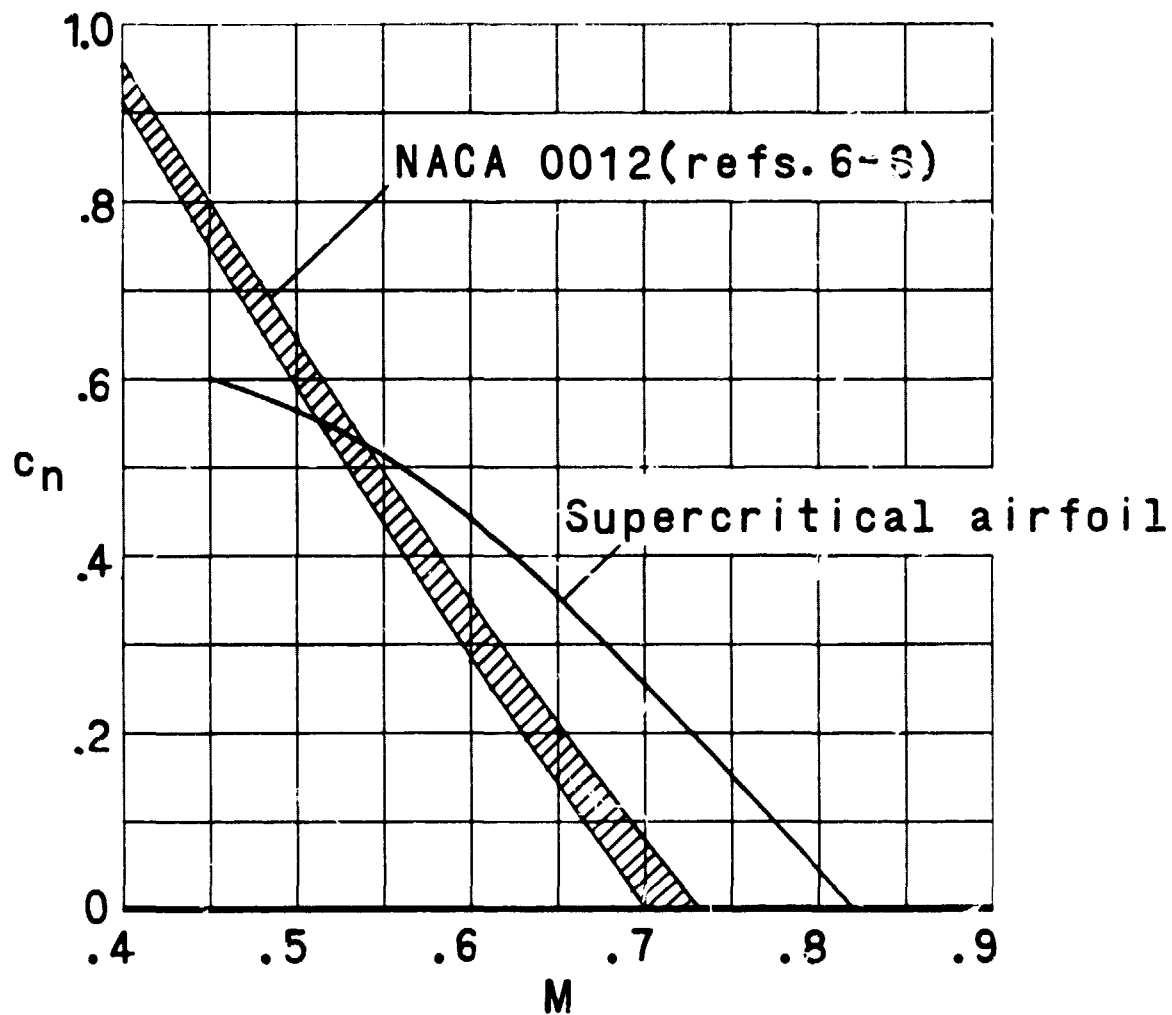
Figure 9.- Variation of drag-rise Mach number with section normal-force coefficient for the supercritical airfoil and the NACA 0012 airfoil.
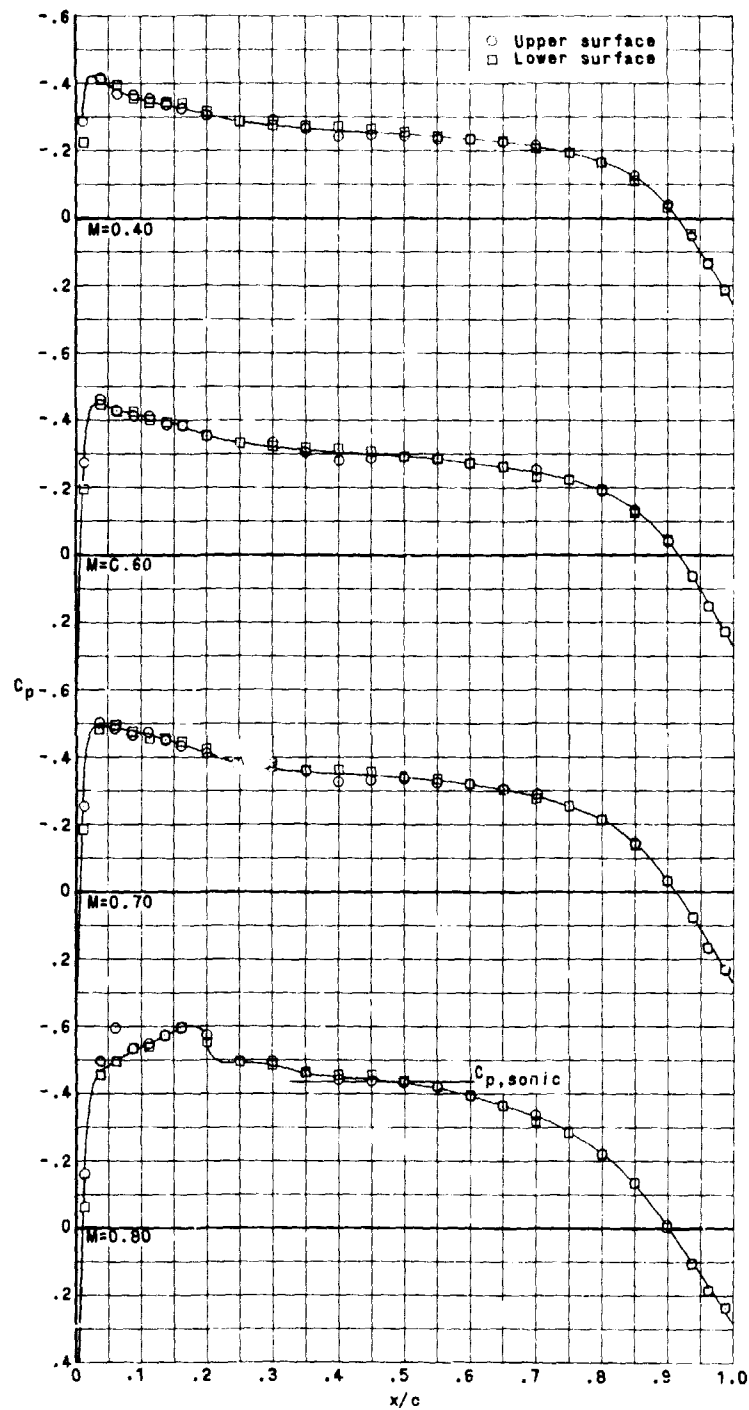
(a) M = 0.40 to M = 0.80.

Figure 10.- Chordwise pressure distributions at α = 0⁰ for Mach numbers from 0.40 to 0.84.
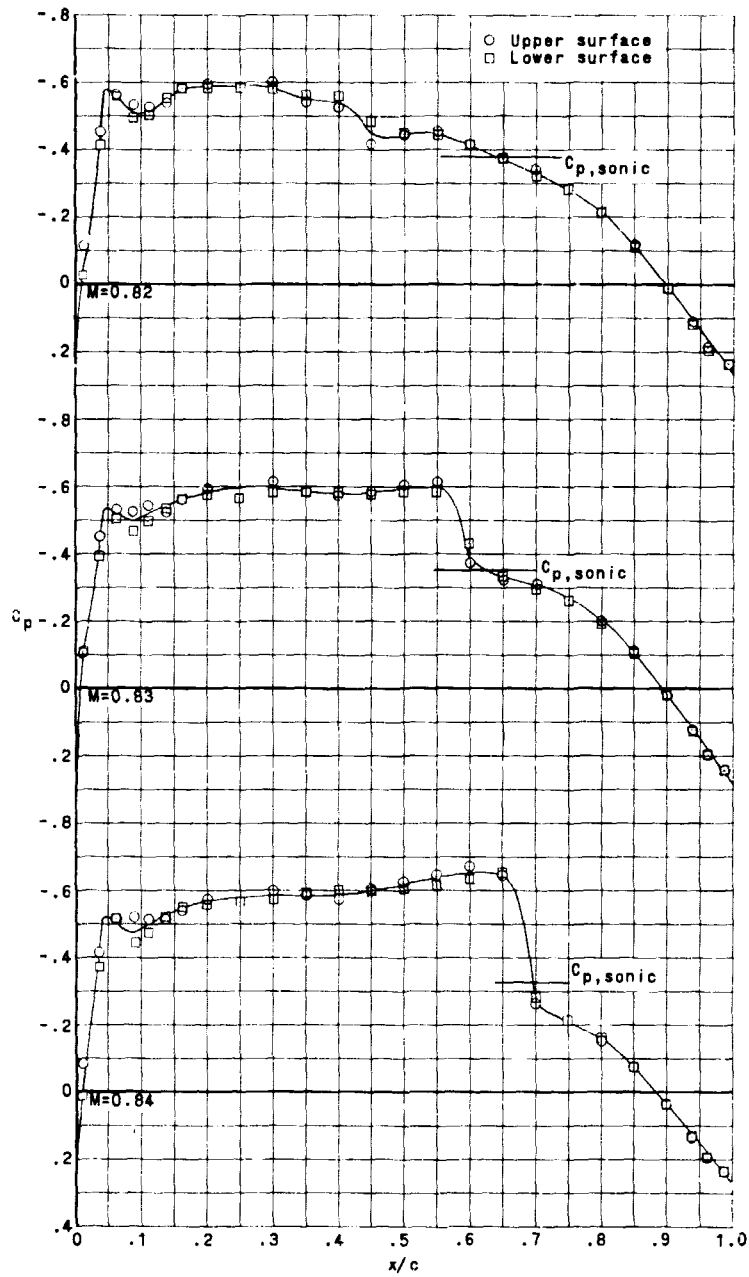
(b) M = 0.82 to M = 0.84.

Figure 10.- Concluded.
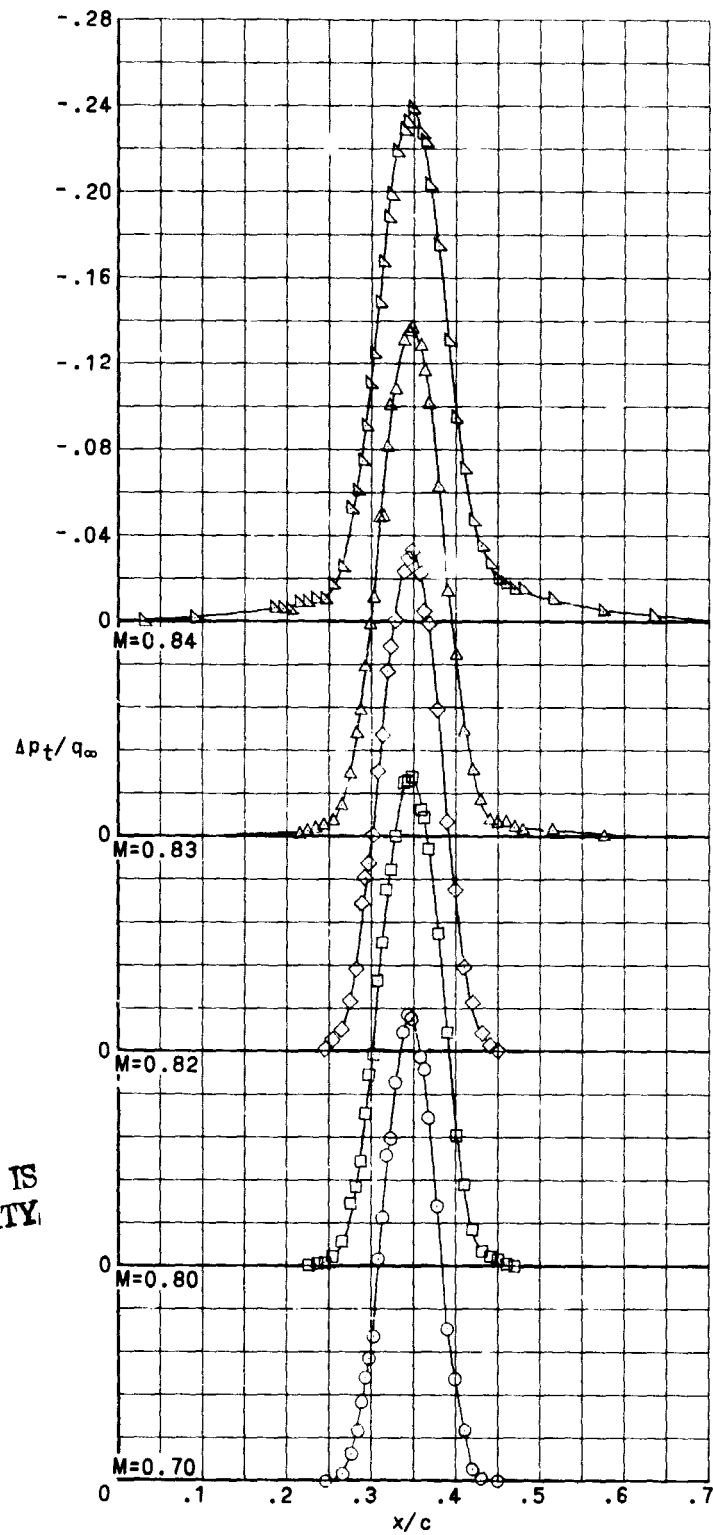
Figure 11.- Wake profiles at $\alpha = 0^0$ for Mach numbers from 0.70 to 0.84.

ORIGINAL PAGE IS OF POOR QUALITY

28

$\Delta p_t / q_\infty$

M=0.84

M=0.83

M=0.82

M=0.80

M=0.70

-.28
-.24
-.20
-.16
-.12
-.08
-.04
0

0   .1   .2   .3   .4   .5   .6   .7

x/c

Figure 11.- Wake profiles at $\alpha = 0^0$ for Mach numbers from 0.70 to 0.84.

28

M=0.40   M=0.60   M=0.70
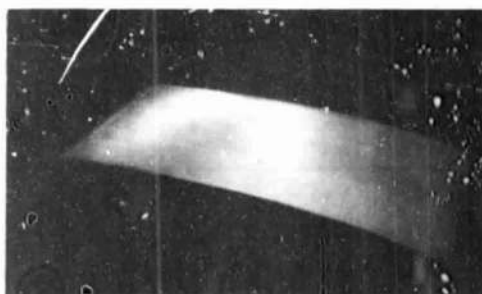
M=0.79   M=0.80   M=0.82

M=0.83   M=0.84   M=0.85

29
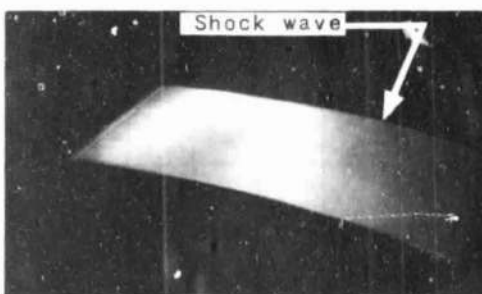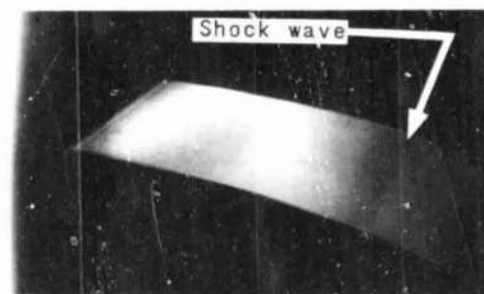
Figure 12.- Oil-flow photographs at $\alpha = 0^0$ for Mach numbers from 0.40 to 0.85.

L-69-1361
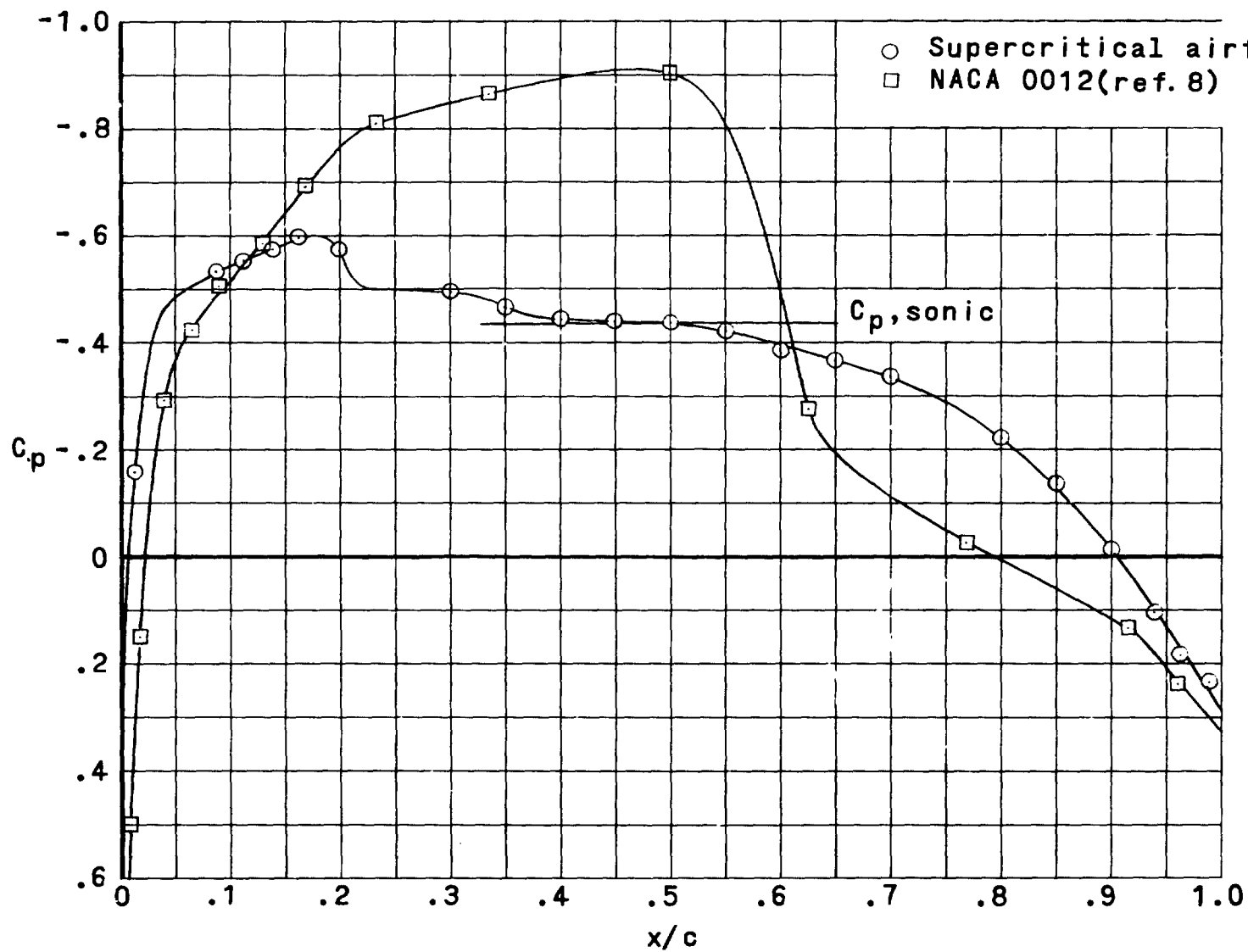
Figure 13.- Comparison of chordwise pressure distributions for the supercritical airfoil and the NACA 0012 airfoil at M = 0.80 and α = 0°.
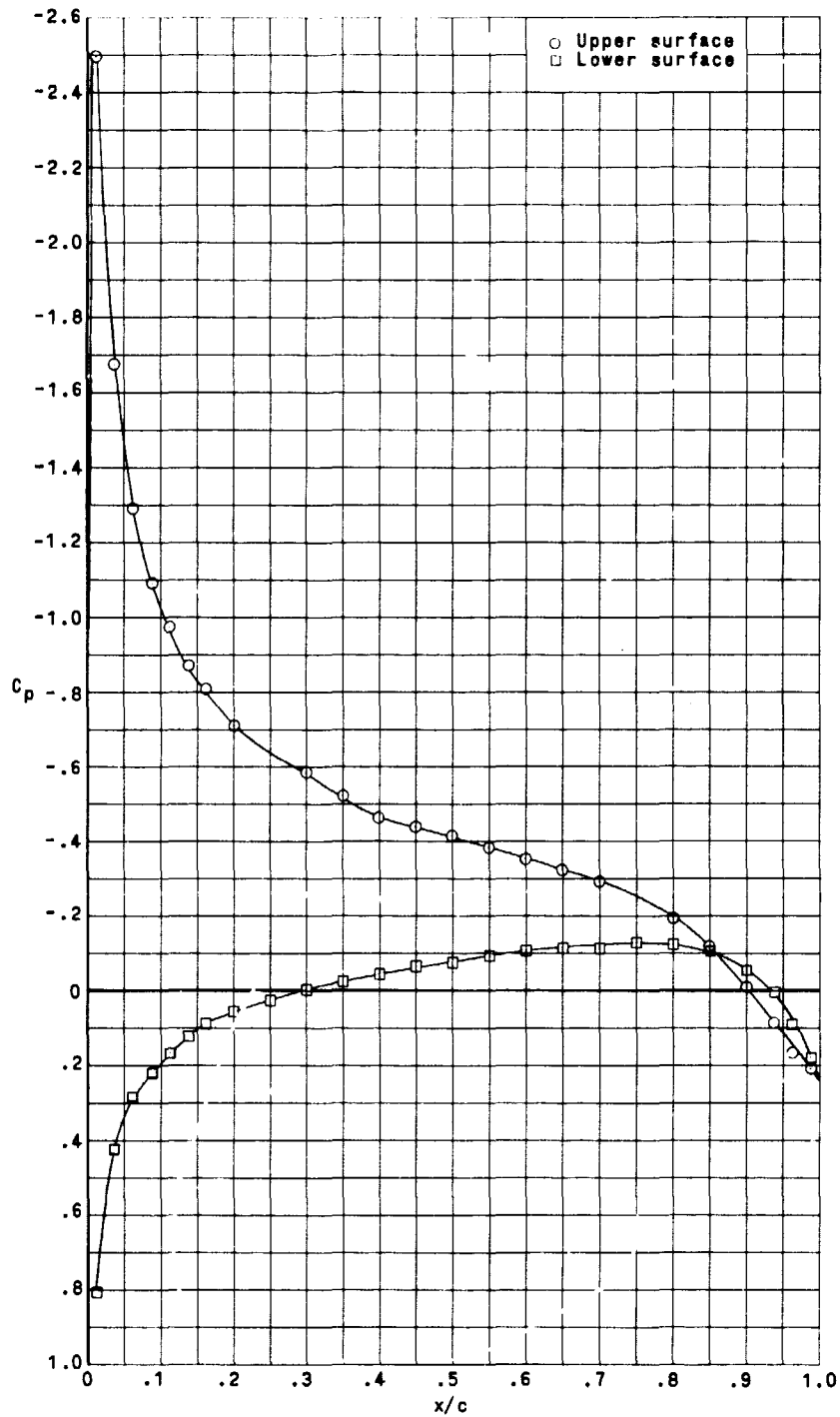
(a) M = 0.40.

Figure 14.- Chordwise pressure distributions at α = 5.5° for Mach numbers from 0.40 to 0.74.
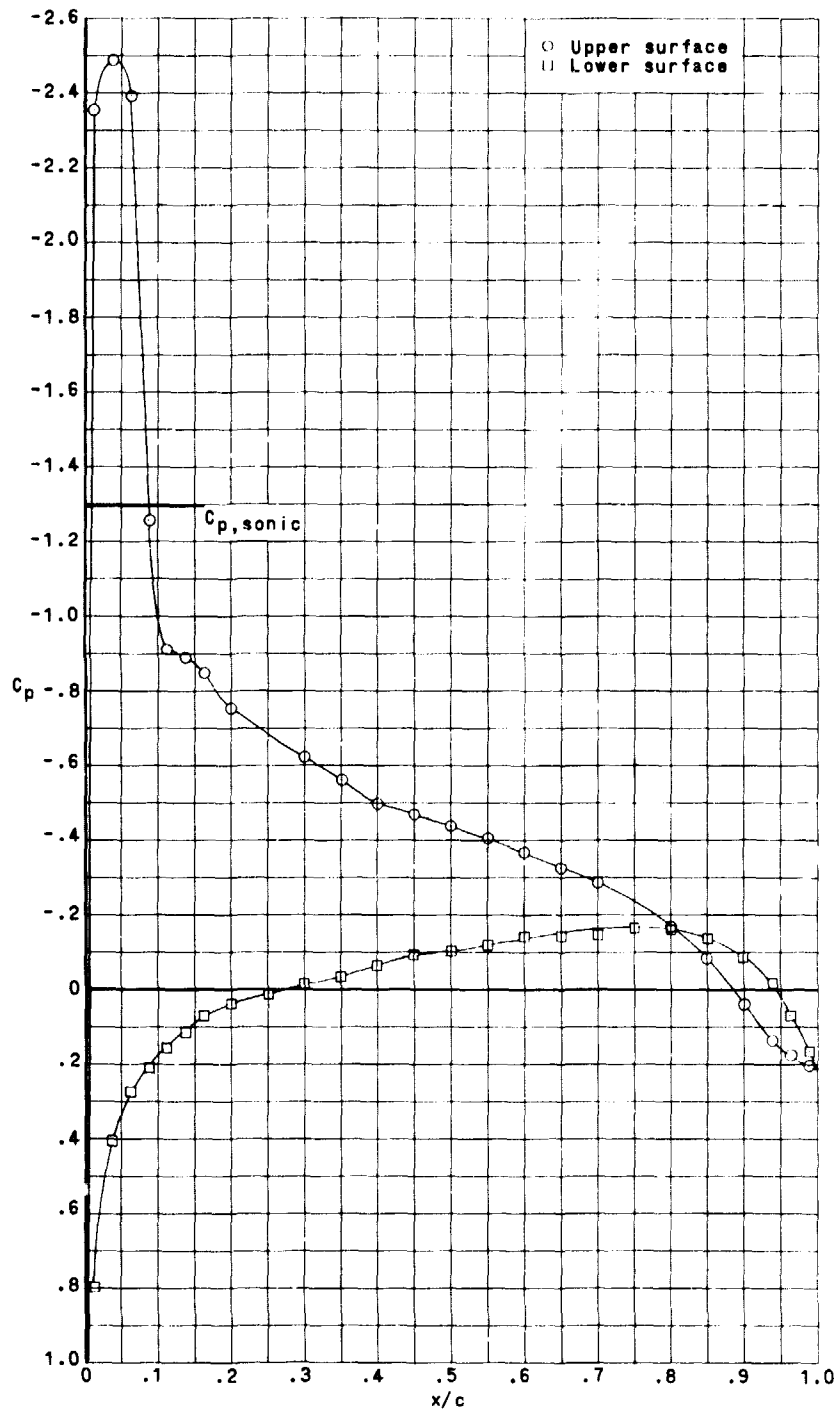
(b) M = 0.60.

Figure 14.- Continued.
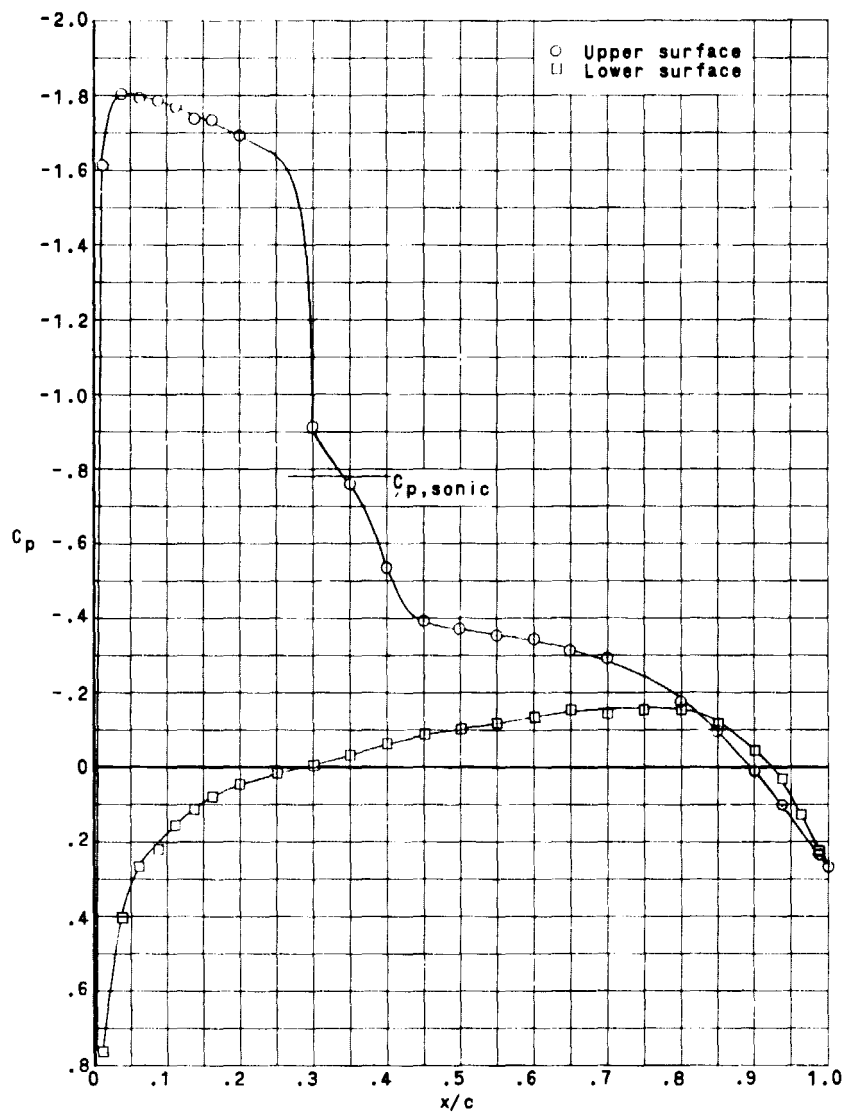
(c) M = 0.70.

Figure 14.- Continued.
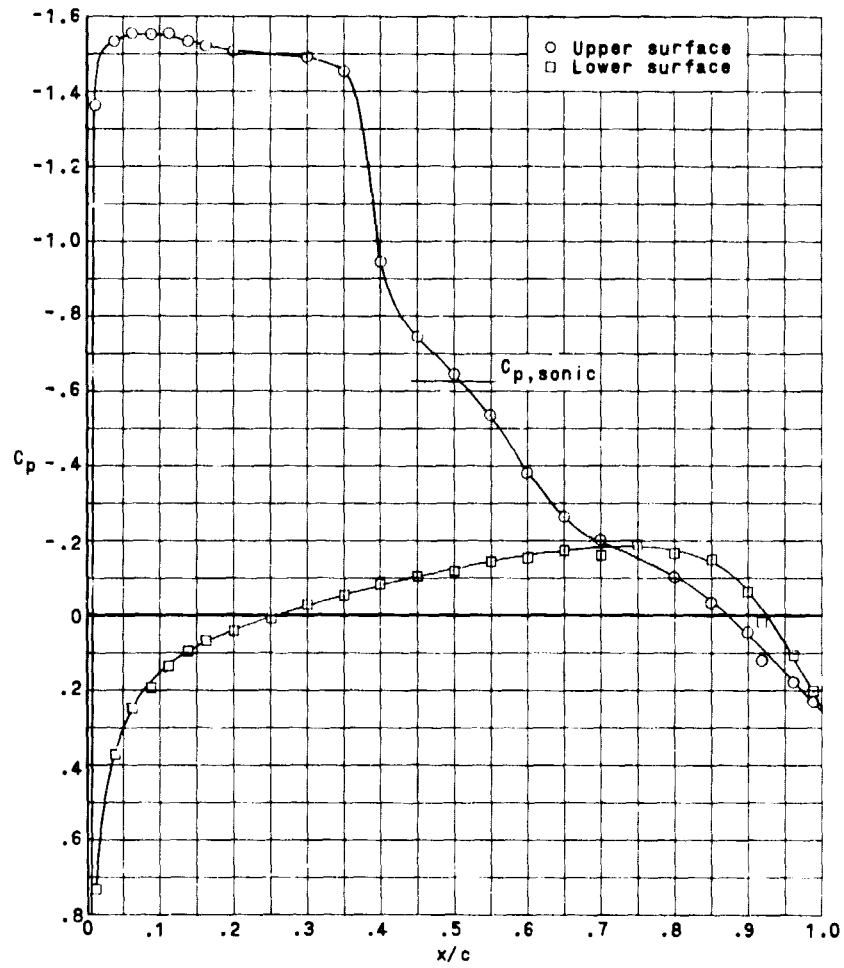
(d) M = 0.74.

Figure 14.- Concluded.
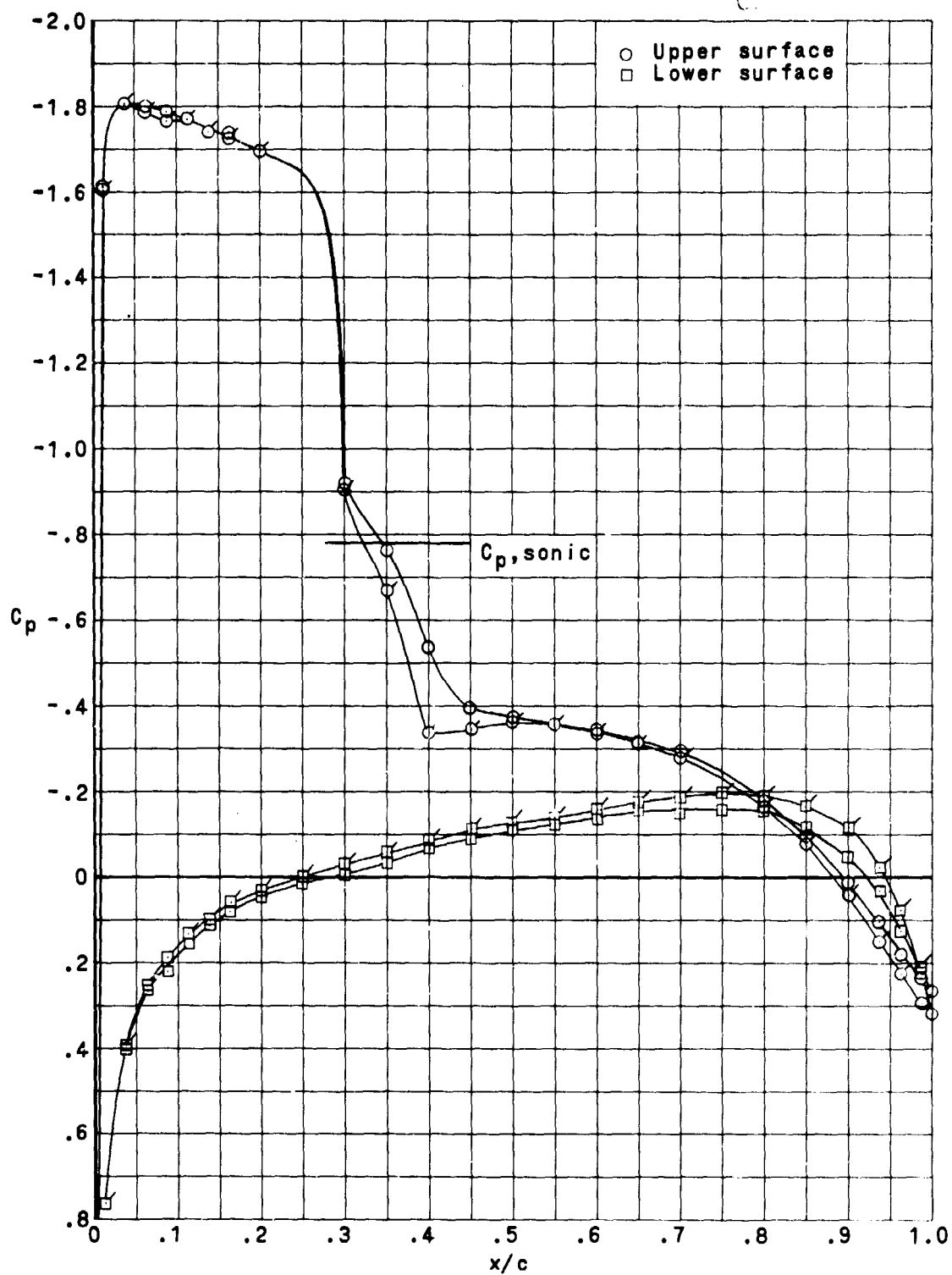
Figure 15.- of boundary-layer transition on the airfoil chordwise pressure distribution. M = 0.70; α = 5.5°. (Plain symbols indicate artificial transition on and flagged symbols indicate natural transition.)

OR'G.... ....
OF PU.. ....

(a) $\alpha = 0^0$ to $\alpha = 2^0$.
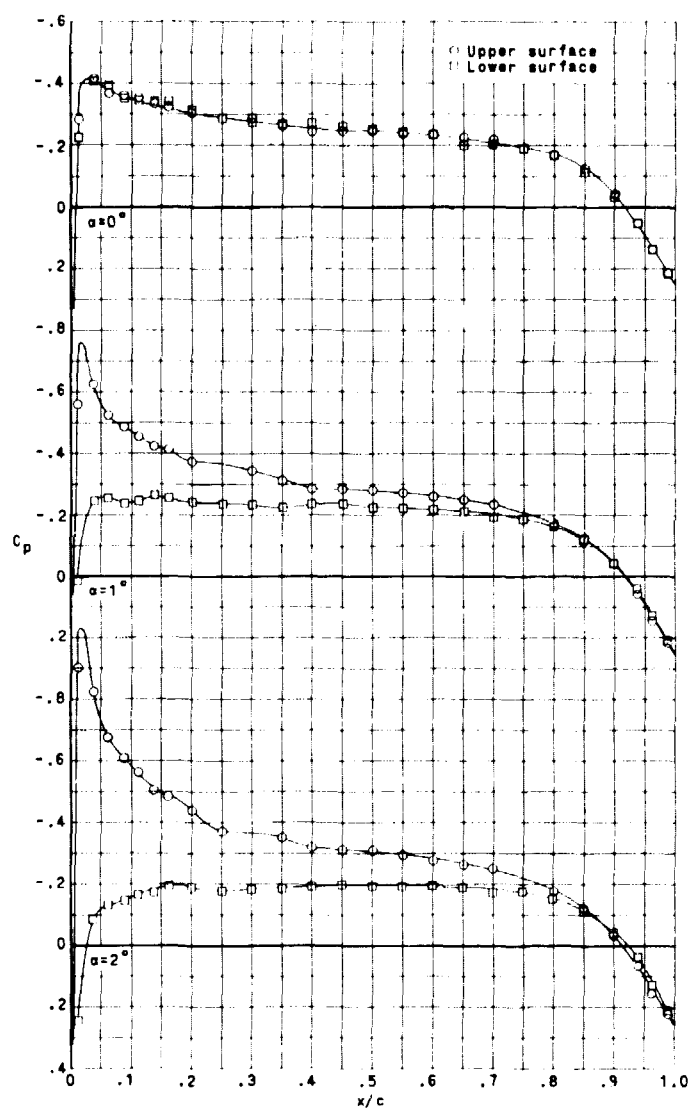
Figure 16.- Chordwise pressure distributions at $M = 0.40$ for angles of attack from 0^0 to 10.5^0.
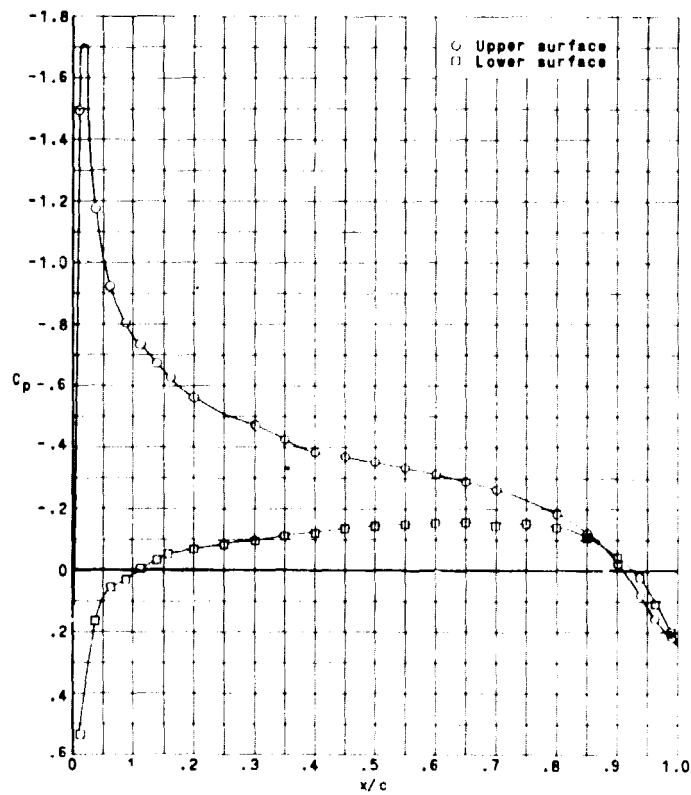
(b) α = 3.5°.

Figure 16.- Continued.
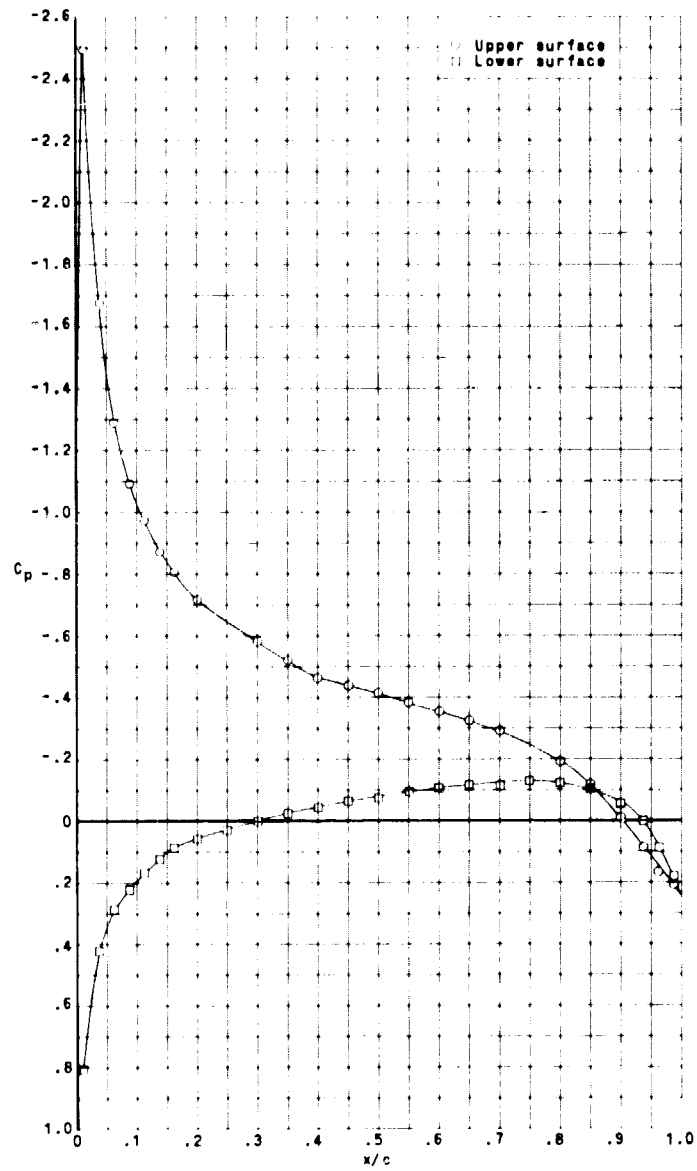
(c) $\alpha = 5.5^\circ$.

Figure 16.- Continued.

(d) $\alpha = 8.5°$.
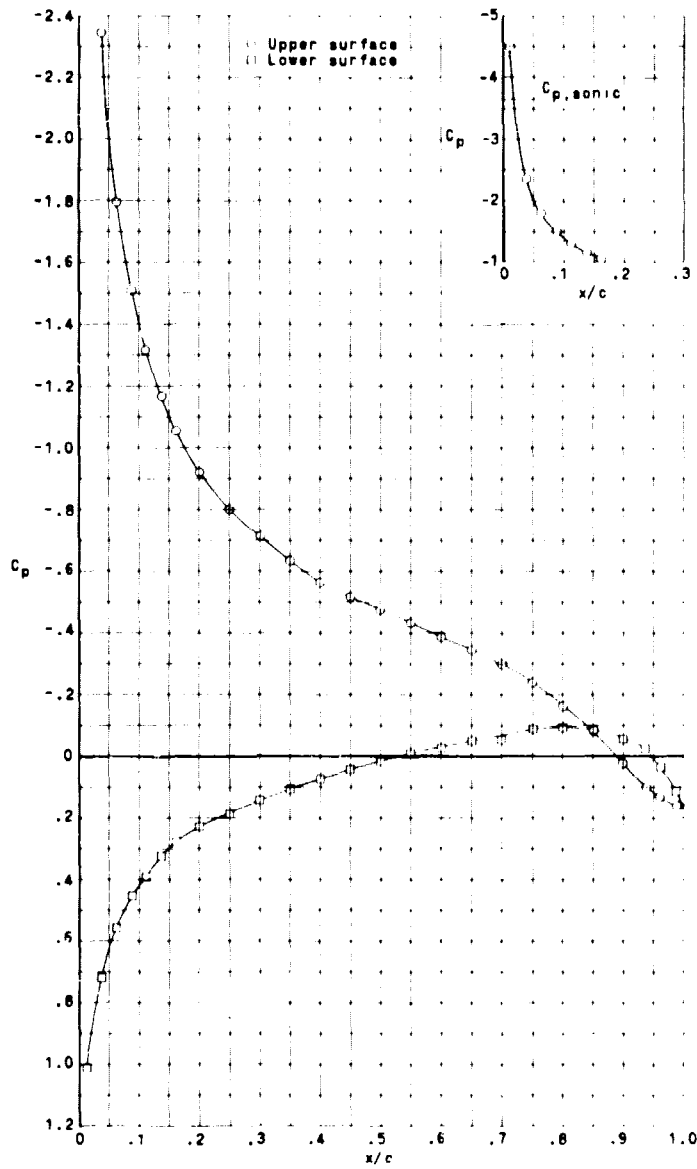
Figure 16.- Continued.
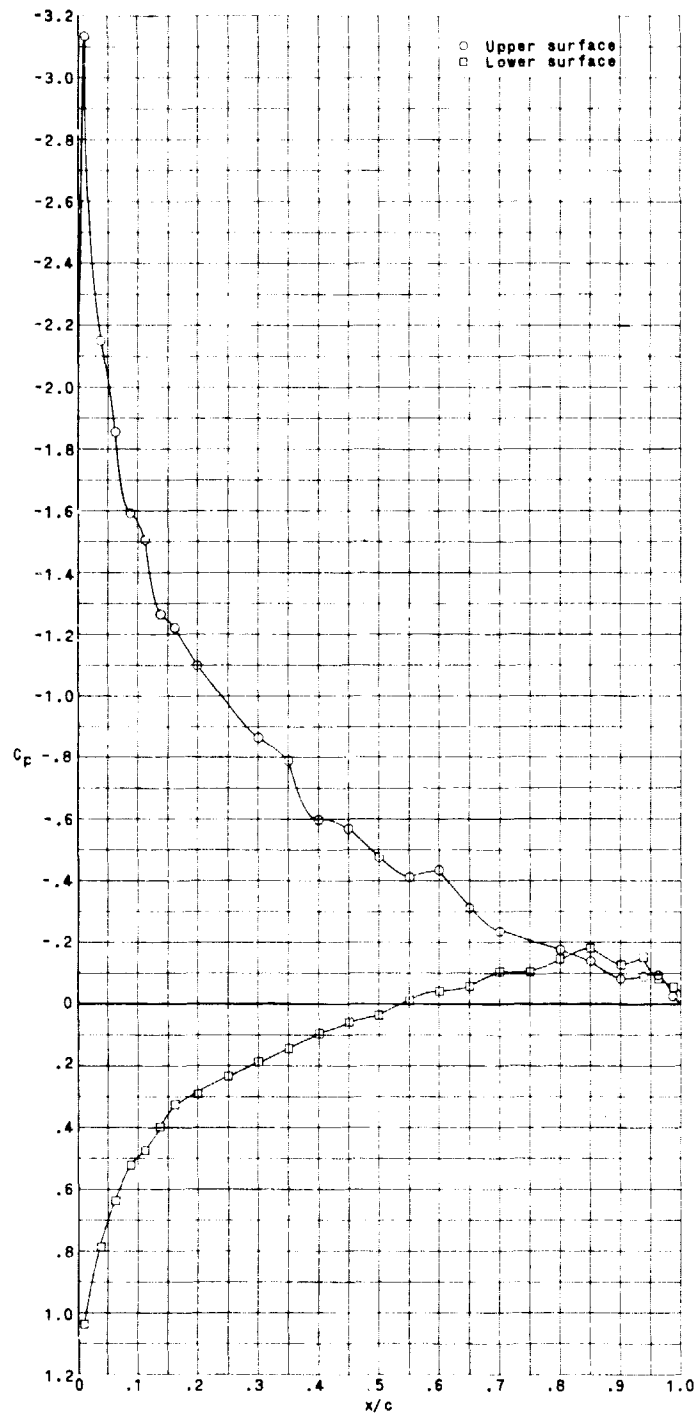
(e) $\alpha = 10.5°$.

Figure 16.- Concluded.